Radiocarbon dating distal tephra from the Early Bronze Age Avellino eruption (Eu-5) in the coastal basin of southern Lazio (Italy) uncertainties, results, and implications for dating distal tephra

Sevink, J.; Bakels, C.C.; Hall, R.L. van; Dee, M.W.

Quaternary Geochronology 63 (2021) 101154

Contents lists available at ScienceDirect

Quaternary Geochronology

journal homepage: http://www.elsevier.com/locate/quageo

Radiocarbon dating distal tephra from the Early Bronze Age Avellino eruption (EU-5) in the coastal basins of southern Lazio (Italy): Uncertainties, results, and implications for dating distal tephra

J. Sevink [a,*], C.C. Bakels [b], R.L. van Hall [a], M.W. Dee [c]

[a] Institute for Biodiversity and Ecosystem Dynamics (IBED), University of Amsterdam, Netherlands
[b] Faculty of Archaeology, Leiden University, Netherlands
[c] Centre for Isotope Research (CIO), Groningen University, Netherlands

ARTICLE INFO

Keywords:
Tephrochronology
Radiocarbon dating
Bayesian analysis
Sampling error
Avellino eruption
Tephra toxicity
Central Italy

ABSTRACT

Distal tephra from the major Somma-Vesuvius Avellino (AV) eruption is widespread in the coastal basins of Southern Lazio (Central Italy). Dated to 1995 ± 10 cal yr BC in 2011, later on doubts arose about the reliability of this frequently cited age. This led to a major effort to date AV tephra holding sections, based on a thorough methodological approach.

Various aspects were studied to identify sections yielding reliable ^{14}C ages, including bioturbation, inbuilt age, and variable sediment accumulation rate. Lowered rates upon deposition of tephra, particularly in anoxic marshy environments and attributed to toxic F contents, showed up as sharp increases in pollen density. The 'sampling error' was quantified for specific sedimentary environments and derived from coring data and published data on accumulation rates for similar Central Mediterranean sites. Next, two Bayesian analyses were performed, a traditional using the full set of samples and a novel, based on samples that were deemed as suitable (no bioturbation, inbuilt age, etc.) and of which the age was corrected for the sampling error.

The age obtained by the novel analysis had the smallest range (1909–1868 cal yr BC), differs about a century, and is virtually identical to the ages published by Passariello et al. (2009) and Alessandri (2019). The earlier found age (2011) is ascribed to a statistical coincidence. The results solve a long debate on the age of the AV eruption, which is the youngest of the three major eruptions in the Central Mediterranean Bronze Age. Ages of the other two, the Agnano Mt Spina (Phlegrean) and FL eruption (Etna), are still uncertain and disputed. This study illustrates the need for a thorough approach in ^{14}C dating tephra holding sediment archives in the Central Mediterranean, and employed a methodology that can be applied in such approach. Attention is called for potentially toxic fluorine concentrations in Campanian tephra, which may have had a serious impact on the contemporary environment and induced chronological hiatuses, but hitherto were not reported for the early tephra.

1. Introduction

The Avellino eruption of the Somma-Vesuvius counts among the major Holocene eruptions in the Central Mediterranean (see Zanchetta et al., 2011) and resulted in 'Pompeii type' sites close to the volcano, where the Avellino tephra covers an exceptionally well conserved Early Bronze Age landscape (see e.g. Albore Livadie, 1999; Vanzetti et al., 2019). These sites were discovered shortly before the end of the 20th century (Albore Livadie et al., 1998) and gave rise to numerous excavations (see e.g. Albore Livadie et al., 2019; Di Vito et al., 2019; Vanzetti et al., 2019. These allowed for a deep insight into the contemporary prehistoric cultures and their land use. The relevance of this eruption for paleoclimatic archives lies particularly in the wide distribution of its tephra and the associated possibilities for long distance correlation. It is enhanced by its specific chemical and mineralogical signature that allows for its easy recognition (see Zanchetta et al., 2011 and 2019). This is exemplified by identification of the Avellino tephra in well known cores from locations as far apart as Lago d'Accesa, in Tuscany (Magny et al., 2007), Lago Grande di Monticchio, in Basilicate (Wulf et al., 2004), Lake Veliko jezero, in Croatia (Razum et al., 2020), Lake Ohrid

* Corresponding author. IBED, Sciencepark 904, 1098, XH, Amsterdam, Netherlands.
E-mail addresses: j.sevink@uva.nl (J. Sevink), C.C.Bakels@arch.leidenuniv.nl (C.C. Bakels), R.L.vanHall@uva.nl (R.L. van Hall), m.w.dee@rug.nl (M.W. Dee).

https://doi.org/10.1016/j.quageo.2021.101154
Received 18 May 2020; Received in revised form 24 December 2020; Accepted 27 January 2021
Available online 5 February 2021

and Lake Shkodra, both in Albania and Montenegro (Wagner et al., 2008; Sulpizio et al., 2010; respectively), and the Sea of Marmara, in Turkey (Çağatay et al., 2015).

Early radiocarbon dating attempts focused on pre-eruption materials found at proximal sites and dating from immediately before the eruption, which was mainly because of the uncertainty about the length of time over which these sites remained uninhabited after the eruption. It also explains why the most accepted age (3.86 ± 0.03 cal Ka BP) was based on radiocarbon analyses of a goat that was killed by the eruption (Passariello et al., 2009). Radiocarbon datings from truly distal areas, based on multiple samples from sedimentary sequences with an intercalated Avellino tephra layer and a Bayesian approach, did not exist till the discovery and dating of such layer in the Agro Pontino (see Fig. 1). It was identified as a tephra layer from the EU-5 eruption phase (Sulpizio et al., 2008) and dated to 1995 ± 10 cal yr BC (or 3935–3955 cal yr BP), based on radiocarbon dates for two sites: Migliara 44,5 and Campo inferiore (Sevink et al., 2011).

The age obtained was slightly older than ages published in previous studies (Albore Livadie et al., 1998: 1880-1680 cal yr BC; Passariello et al., 2009: 1935–1880 cal yr BC) and this led to quite some scientific debate (see for example Jung, 2017). There still is no agreement on its age as is exemplified by Zanchetta et al. (2019) and by the recent study of Razum et al. (2020), in each of which both dates (Passariello et al., 2009; Sevink et al., 2011) are mentioned. This uncertainty led Alessandri (2019) to review all available radiocarbon dates connected with the eruption, of which most stem from proximal archaeological sites, but also include distal sediment sequences. He found a calibrated age that is close to the age found by Passariello et al. (2009): 1929–1856 cal yr BC. Alessandri additionally stressed the importance of the Avellino tephra and its age for the stratigraphy of the Early and Middle Bronze Age in South and Central Tyrrhenian Italy, which has been heralded by many other archaeologists. Remarkably, it is not only the Avellino eruption of which the absolute age is still disputed. The same holds for the Agnano Mt Spina eruption (Phlegrean) and FL eruption (Etna), which are the other two major Bronze Age tephra layers in the Central Mediterranean mentioned by Zanchetta et al. (2019). They state that the 'Agnano Mt Spina chronology is supported by poor radiocarbon dating, which needs to be significantly improved' and that 'The chronological constraints for FL are even less robust'.

A palaeogeographical reconstruction of the Agro Pontino and Fondi basin, focussing on the Bronze Age and using the Avellino EU-5 tephra layer (further referred to as the AV layer) as a marker bed, is a central topic in the Dutch Avellino Impact Project, which started in 2015. Results from this project were published in a number of papers (Doorenbosch and Field, 2019; Van Gorp and Sevink, 2019; Van Gorp et al., 2020; Sevink, 2020), and include a recent paper on the identification and characteristics of Bronze Age tephra in these basins (Sevink et al., 2020b). Apart from the AV layer, these comprise far less common and thinner tephra layers, ascribed to the earlier Phlegrean Astroni6 and the later Somma-Vesuvius AP2 tephra. Radiocarbon ages that were obtained for samples from directly below the AV layer in the Agro Pontino and Fondi basins (Sevink et al., 2020b) varied little and converged to c. 3570 yr BP, conforming to results for proximal sites (e.g. Passariello et al., 2009; 2010; Albore Livadie et al., 2019; Alessandri, 2019). However, samples from above this AV layer exhibited a much larger variation in radiocarbon age, which was rather surprising and could not be straightforwardly explained. These results raised serious questions about the reliability of the earlier established age of the AV layer in the Agro Pontino (Sevink et al., 2011), which were analogous to questions that had been raised by Jung (2017) and Alessandri (2019). It led us to a critical evaluation of the radiocarbon dating of the AV layer, paying attention to aspects that thus far had not been considered in such studies of distal sites.

In the first place, in most Bayesian analyses that served to date intercalated tephra layers in sediment archives it is implicitly assumed that the sedimentation rate was constant. An example is the dating of the AV layer by Sevink et al. (2011). However, evidence that such assumption is valid is often scant and our results strongly suggested that in several of the sections studied a more or less significant stratigraphic hiatus or decline in the sedimentation rate had occurred upon tephra deposition. This seriously hampers a straightforward application of a Bayesian analysis and led us to the following connected questions: 1)

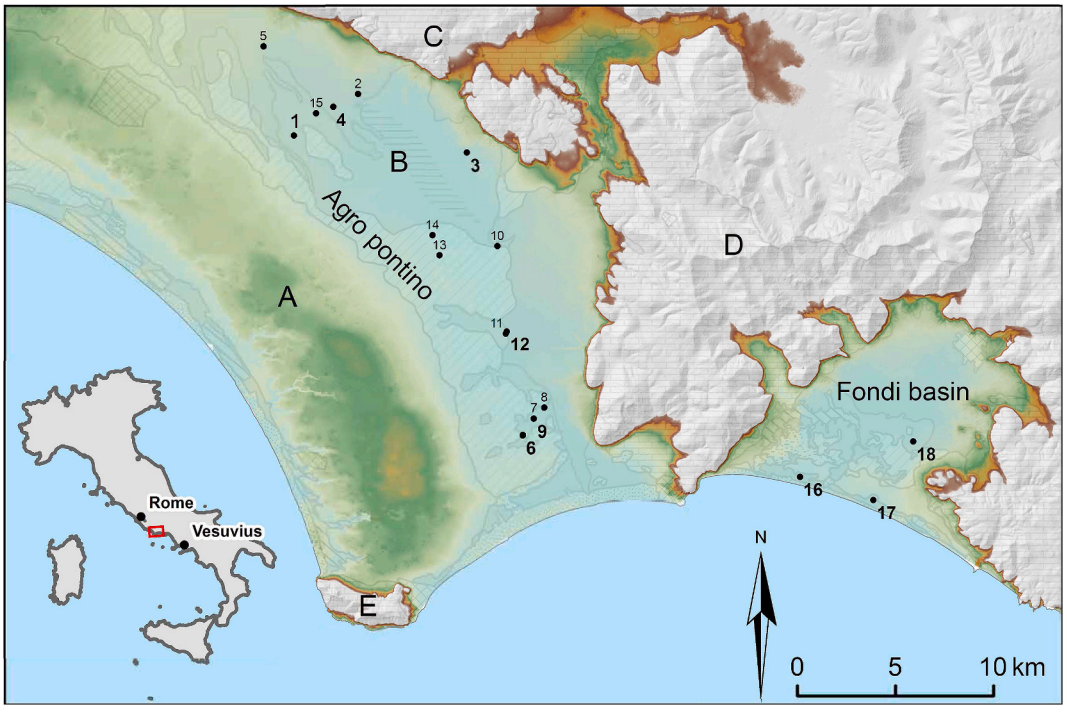

Fig. 1. Location of the Agro Pontino and Fondi basin, and of the sites studied. Numbers refer to sites described in Table 1. Numbers of locations with palaeoecological data are in bold. A = higher complex of Pleistocene marine terraces; B = Agro Pontino graben; C = Monti Lepini; D = Monti Ausoni; E = Monte Circeo.

What evidence may exist for the occurrence of a post-tephra stratigraphic hiatus/lower sedimentation rate? And 2) What might be the cause of such hiatus/lower sedimentation rate? We tried to answer both questions; the first by studying pollen densities in representative sections, which is a technique that has often been used for the identification of changes in sedimentation rates (see for example Maher, 1972); the second by paying attention to the potentially toxic impact of tephra on ecosystems/vegetations (see for example Grattan and Pyatt, 1994).

Another aspect is that lagoonal/lacustrine sediments in the Mediterranean generally are low in materials that are suitable for reliable radiocarbon dating (such as from non-aquatic plants, see Sevink et al., 2013). In such situations, the 'sampling error' may become significant, being defined as the difference in age between the material that was sampled and dated, and the tephra layer. This difference is determined by the vertical distance between the two and the sedimentation rate but generally values for the latter are rather uncertain. A further complication is that seeds and other plant materials are selected from individual samples, which have a certain thickness, thus introducing further uncertainty in the sampling error. In particular in environments with low sedimentation rates and scarce suitable plant macro remains, for which large samples need to be taken for the retrieval of the material required for radiocarbon dating, this 'error' may easily be in the order of 100 years ±50 years. In most studies that aim to date tephra from this type of sedimentary environment little attention is paid to this sampling error, but it can be accounted for in a dedicated Bayesian analysis, that also considers variations in sedimentation rates.

Based on answers obtained for the two questions described above, from a larger set of sites we selected those sites with stratigraphies/ecosystems that were least affected by a toxic impact of the tephra deposited and lacked indications for a significant change in sedimentation rate upon tephra deposition. On these selected sites we performed such dedicated Bayesian analysis, which included a check of the effect of the 'sampling error'. Results are reported in this paper and solve the still existing controversy about the age of the Avellino eruption. Additionally, we discuss the relevance of our seemingly novel methodological approach for solving uncertainties in tephra ages for similar sediment archives.

2. General information and backgrounds

During the last glacial period, when sea level was very low, in the Agro Pontino and Fondi basin rivers cut deep valleys into a thick complex of predominantly fine-textured Quaternary sediments (e.g. Sevink et al., 1984), of which the youngest were described as the Borgo Ermada marine complex. These valleys gradually filled in with the Holocene sea level rise. Deposits from this Holocene transgression were described as the Terracina marine complex. Towards c. 2 ka BC, when sea level rise slowed down (Lambeck et al., 2011; Vacchi et al., 2016), beach ridges could build up and lagoons came into existence (Sevink et al., 1982, 1984; Van Gorp and Sevink, 2019; Van Gorp et al., 2020). Near the coast, these were mostly freshwater lagoons, which overall were shallow and underlain by sandy beach ridge deposits, while further inland the lagoons graded into marshy valleys.

In the central part of the Agro Pontino basin a different situation existed. Upon sea level rise the Amaseno river built up an alluvial fan, which shortly before the AV eruption started to block the single outlet of the fluvial system that drained the northern part of this basin (see AF in Fig. 2). This led to a gradual 'drowning' of the earlier inland landscape and created a large lake and associated marshes (Van Gorp and Sevink, 2019; Van Gorp et al., 2020). In the NE part of this lake, peat with intercalated lacustrine marls (calcareous gyttja) and some travertine accumulated, and in the SW pyritic black organic clays. In the NW, these lacustrine deposits graded into fluvio-deltaic sediments and, further upstream, genuine fluvial sediments. The waters that ran into the lake from the adjacent mountains were largely fed by springs with highly calcareous and often sulphuric waters (Boni et al., 1980; Tuccimei et al., 2005; Sappa et al., 2014). A similar situation existed in the Fondi basin, where an inland lake formed also with Holocene peats and calcareous gyttja.

Agro Pontino: CL = coastal lake; IL = inland lake. AF = Amaseno fan. 1/2 = oxic lacustrine/lagoonal sediments and 3 = anoxic lacustrine sediment with shaded transitional zone; 4 = fluvio-deltaic sediments. Fondi basin: 1/2 = oxic lacustrine/lagoonal sediments; 4 = fluvio-deltaic and alluvial sediments. Pt = Pleistocene deposits; B = beach ridges. Arrows indicate former river courses. Tentative boundary indicated with ————. Boundary between coastal and inland lake is indicated in red.

The AV tephra fell into these waters and wetlands, to form a very

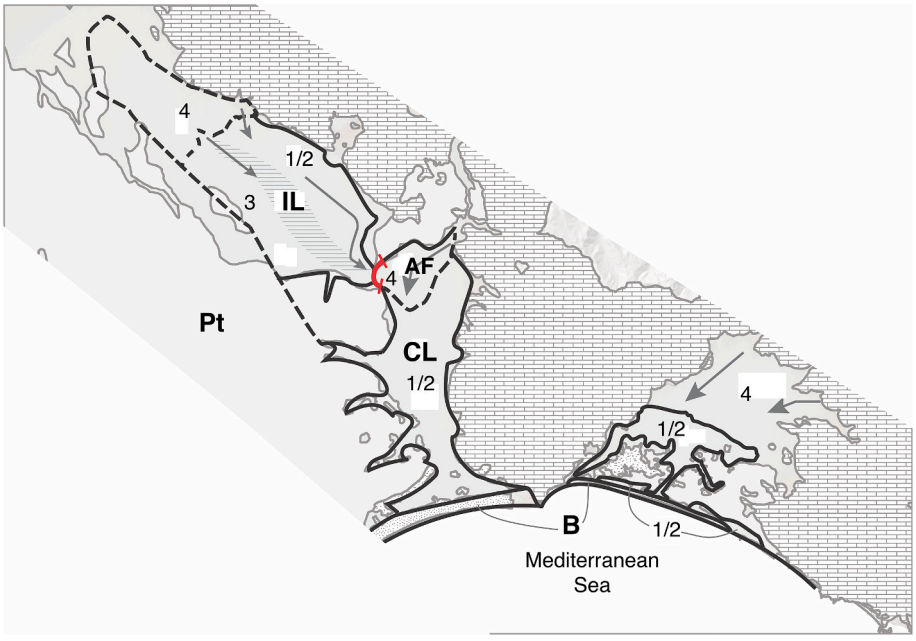

Fig. 2. Landscape Southern Lazio c. 2000 BCE.

conspicuous and easily identifiable tephra layer. It was preceded by tephra from a slightly earlier and smaller Astroni eruption (most probably the Astroni 6 eruption, see Sevink et al., 2020b), which seems to be restricted to the Fondi basin and followed by a minor tephra fall from the Monte Somma-Vesuvian AP2 eruption, recorded in the south of the Agro Pontino. Occurrences, characteristics and ages of these three tephra are extensively described in Sevink et al. (2020b). The age of the AP2 tephra is less well known than that of the Avellino eruption, its most recently published age being c. 1700 cal yr BC (Jung, 2017; Sevink et al., 2020a). The age of the Astroni 6 eruption is rather uncertain. According to Smith et al. (2011) it is slightly younger than 4098–4297 cal yr BP (Astroni 3) and older than 3978–4192 cal yr BP (Fosso Lupara), while Arienzo et al. (2015) report an age of 4.23 cal kyr BP for the Astroni 6 eruption. The latter age is earlier than the age reported by Sevink et al. (2020b), which is in between 2168 ± 118–2117 ± 84 cal yr BC (4118 ± 118–4067 ± 84 cal yr BP), and is more in line with the age reported by Smith et al. (2011).

In the Agro Pontino and Fondi basin, four types of sedimentary environments were distinguished in which the AV layer was encountered (Van Gorp and Sevink, 2019; Sevink et al., 2020b). Type 1: oxic aquatic to marshy, with peat to peaty clay; Type 2: oxic aquatic (lacustrine/lagoonal), with calcareous gyttjas to calcareous marls ('gyttja'); Type 3: anoxic marshy, with pyritic more or less peaty black clays ('pyritic clays'); Type 4: oxic, fluvio-deltaic, with calcareous clays to loams. Their overall distribution is depicted in Fig. 2. In this figure no distinction is made between areas with type 1 and with type 2 sediments, because the intricate pattern in which they occur cannot be depicted at the scale of this figure.

Following on the large scale development of agriculture in Southern Lazio, which started in the Late Bronze Age (Attema, 2017), over large areas these sediments were gradually buried under mostly fine textured, reddish-brown reworked soil material, described as fluvio-colluvial deposits (Sevink et al., 1984), whereas outside these areas peat continued to accumulate, if not stopped by land reclamation and associated drainage (Van Joolen, 2003; Feiken, 2014; Attema, 2017). The overall situation is depicted in Fig. 3.

The AV layer was identified in the field as a 2–3 cm thick intercalated sandy grey-creamy coloured tephra layer. This layer holds very conspicuous idiomorphic 'golden' mica and sanidine crystals, of which the mica reaches sizes up to c. 4 mm. Where the tephra layer is intercalated in gyttja, such as in the interior basin of the Agro Pontino near Mezzaluna and in the coastal lagoonal deposits near Borgo Hermada, it forms a virtually continuous horizontal layer with often sharp upper and lower boundaries, which could be followed over large distances. Though this type 2 sediment holding the AV layer is extremely well suitable for palaeoecological studies, plant macro remains are invariably from truly aquatic plants, potentially affected by reservoir effects, and therefore unsuitable for radiocarbon dating. The pyritic (peaty) clays (type 3) are marked by low sedimentation rates, demonstrated by the shallow occurrence of the AV layer in such sediments – often less than 50 cm below current ground level or below the fluvio-colluvial deposits - and are also low in suitable plant macro remains, posing problems for reliable radiocarbon dating. Aquatic to marshy peats and clays (type 1) hold a more discontinuous AV layer, but these sediments are basically well suitable for radiocarbon dating and palaeoecological studies. Fluvio-deltaic sediments (type 4) were rather unsuitable for palaeoecological studies and radiocarbon dating for a variety of reasons: common hiatuses, discontinuous strata, low pollen content due to oxidative conditions, etc.

Most of the radiocarbon dates were on samples from type 1 sediments. For the palaeoecological studies cores and monoliths were sampled to cover the two basins concerned. These samples allowed for an analysis of the impact of the AV tephra fall on the relevant major types of vegetations encountered. For a study on the potential toxic impact of the tephra, cores were selected to cover the same range of environments (types 1, 2, and 3), but based on the systematic differences in geochemical conditions (oxic versus anoxic/sulphidic; super saturated calcareous waters – non saturated waters). The approach was to assess whether 'spikes' in element concentrations occur in the AV layer and immediately above that layer, which can be linked to the deposition of this tephra, the elements concerned having been immobilized in the specific environment.

3. Methods and materials

For radiocarbon (^{14}C) analysis of samples from immediately above and below tephra layers, plant macro remains were handpicked under the microscope from subsamples that were obtained by sieving over a

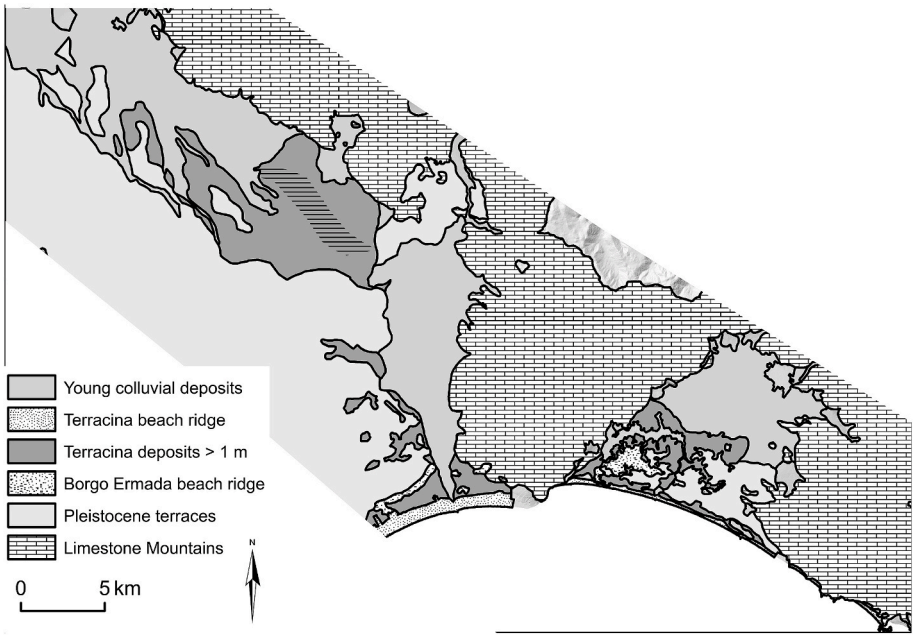

Fig. 3. Simplified geological map of the area studied, showing the distribution of the Holocene Terracina deposits and beach ridge, and the Holocene Young colluvial deposits. > 1 m = thicker than 1 m.

105 or 150 μm mesh sieve to remove fines. Remains from plants that might obtain their carbon dioxide from water were excluded. In some instances, suitable plant macro remains were absent and humic material (black organic clay with very finely divided organic matter) was used. For ^{14}C analysis, samples were subjected to an ABA pre-treatment. Samples were analysed by the AMS-method at the Centre for Isotope Research (CIO) of the University of Groningen, The Netherlands. For an extensive description of the methods and AMS systems (GrA and GrM) used at CIO, see Dee et al. (2020). ^{14}C dates given (in yr BP) are based on the standardized calculations, including correction for isotopic fractionation (Mook and Van Der Plicht, 1999; van der Plicht and Hogg, 2006). Dates have been calibrated using the software OxCal 4.3 (Bronk Ramsey, 2017) and the IntCal13 calibration curve.

For the palaeoecological study, sediment subsamples of 100 cm^3 were wet sieved and plant macrofossils were picked from the resulting residues. For separation of pollen, samples were treated with 10% KOH, 37% HCl, bromoform/ethanol (specific gravity 2.0) and acetolysis. To every sample Lycopodium spores tablets were added for the determination of the pollen concentration. Results for plant macrofossils, pollen and spores have already been published elsewhere (e.g. Bakels et al., 2015; Doorenbosch and Field, 2019) or will be published in the near future. Here, focus is on changes in vegetation upon the deposition of the AV tephra inferred from the pollen assemblages encountered and in pollen concentration as indicator for changes in sediment accumulation rate.

Thin sections of undisturbed samples for microscopic study were produced at the RCE (Amersfoort, The Netherlands) by impregnation with resin, followed by cutting and polishing to a thickness of ca. 30 μm. Sections were studied under a petrographic microscope.

For chemical analysis of potentially toxic elements, cores were taken with a gouge auger at sites with a distinct AV layer. Core sections of 10–12 cm length were cut into 5 to 6 samples that were each 2 cm thick, with the tephra-bearing layer being one of the central layers. From each sampled layer 250 mg was transferred to a 50 ml Teflon PFA microwave vessel and 6 ml HCl 37% and 2 ml HNO_3 65% was added. The samples were left to react for 60 min before digestion in a microwave (Multiwave 3000, Anton Paar GmbH, Ostfildern, Germany). The sample was then transferred to a 50 ml volumetric flask and after addition of 1 ml of lanthanumnitrate (3.1 g $La(NO_3)_3$ in 100 ml water) diluted to the mark using 18 MΩ-water. The whole procedure was performed in duplicate. Trace elements (Zn, Pb, Hg, Cr, V, Cu, Sr) were measured in triplicate using an ICP-OES (Optima-8000, PerkinElmer, Waltham, U.S.A.). Analyses were performed at the IBED lab (University of Amsterdam).

Fluorine contents were estimated at Actlabs (Canada) by FUS-ISE. Samples 0.2 g in size were fused with a combination of lithium metaborate and lithium tetraborate in an induction furnace. The fuseate was dissolved in dilute nitric acid and prior to analysis by ISE the ion strength of the solution was adjusted. The chloride ion electrode is immersed in this solution to measure the fluoride-ion activity directly. The detection limit for F was 0.01%. Actlabs also performed a full chemical analysis of sample 192 using procedures and techniques which are similar to the one described above.

Bulk densities of undisturbed core segments were established by drying and subsequent weighing of samples of known volume. After treatment with H_2O_2 and HCl to remove organic material and calcium carbonate, respectively, the weight percentage of the fraction >20 μm was established. Samples were sieved over a 63 μm sieve. Silt and clay fractions in the remaining suspension were estimated with a sedigraph (Sedigraph III Plus, Micromeritics, Norcross, USA). Tephra contents were defined as the fraction >63 μm, since that fraction was found to be dominantly composed of tephra particles (see also Sevink et al., 2020b).

Post-Avellino mean sediment accumulation rates for the various sites and cores studied were estimated using all available information (archaeological, chronometric) on the age and phasing of the younger, anthropogenic fluvio-colluvial sediments that were encountered in the sections concerned (see e.g. Van Joolen, 2003; Feiken, 2014). Additionally, for a small number of sites holding two tephra layers (AV layer and either tephra from the Phlegraean Astroni eruption or the Vesuvian AP2 eruption), mean accumulation rates could be estimated based on the ages of these tephra layers and thickness of the intercalated sediment. Lastly, for comparison accumulation rates for other Central Italian sites were taken from published cores.

4. Results and discussion

Sections that were obtained with a gouge corer, by digging a pit, or from existing pits are indicated in Fig. 1. An overview of the various sections and their major characteristics is presented in Table 1, while Table 2 shows the results from the ^{14}C dating for relevant samples. A full overview of samples for which ^{14}C dates are available is given in appendix A. First, attention will be paid to the dates and the potential factors that play a role. These factors will be dealt with individually, discussing their potential role in the sections studied and the relevant analytical results. The objective is to assess the value of each of the dates and how they might best be incorporated in the Bayesian chronological analysis (Bronk Ramsey, 2009).

4.1. ^{14}C dates: first evaluation

In Table 2 an overview is given of the dates for samples that may provide reliable indications of the age of the AV layer. To facilitate the discussion, samples from below and from above the AV layer are separately presented. Additional information presented in this table concerns aspects that are dealt with later on and pertain to factors that limit their suitability for the Bayesian analysis, and the sampling error. For details on the Bayesian analyses, reference is made to Appendix B, while OxCal codes used can be found in Appendix C.

The dates for materials from below the AV layer at first sight provide a precise and reliable *terminus post quem* for this tephra, given the fact that 10 of the 14 samples analysed were close to the previously published age (Sevink et al., 2011). The exceptions are from the sites of Frasso 500 (500), Femmina Morta (197), and Mezzaluna (405). For the Femmina Morta site, the set of ^{14}C ages for the various samples (see appendix A) strongly suggests that the latter two dates concern younger materials that for some reason were present in the sediment underneath the AV layer (for a full discussion see 4.2). The date for Mezzaluna concerns wood from an older tree trunk (at 10 cm below the AV layer) and its higher age is therefore not surprising.

A factor not accounted for is the aforementioned sampling error, which combines the accumulation rate and depth of sampling relative to the AV layer. It represents the offset in age between the sedimentary layer from which the ^{14}C date was obtained and the tephra layer. At Mesa for example, the sample was from 0 to 3 cm below the AV layer, which assuming an accumulation rate of 3 cm/century would imply that the AV layer is between 0 and 100 years younger. Whether this rate is realistic will be discussed in section 4.4, as well as the potential impact of such an error.

For the samples from above the AV layer, already at first sight it is clear that the ^{14}C ages obtained for the samples from Migliara 44.5 and Campo inferiore are unexpectedly high and the result for Mesa too young to be consistent with the rest of the dates in Table 2. A number of causes can be distinguished for the wayward dates, several of which have already been mentioned in section 2. These include bioturbation, the old wood effect and the sampling error, being dependent on the accumulation rate and thickness of layers sampled for extraction of material to be dated.

4.2. Bioturbation

For most sections, the ^{14}C dating was performed on a small number of plant macro remains of limited size, with emphasis on seeds and small plant remains (twigs, small branches and leaves). Downward transport

Table 1
General data on the sites studied. Numbers in the column 'Nr. In Fig. 1' refer to locations indicated in Fig. 1. Facies: A = anoxic pyritic clay (type 3); P = oxic peat/peaty clay (type 1); G = oxic gyttja (type 3); F = oxic fluvio-deltaic clays/loams (type 4). AV = Avellino EU5 tephra layer; Astr = Astroni tephra layer (presumably Astroni 6); AP2 = Vesuvian AP2 eruption. X = data available; (x) = unreliable dating (see Table 2); - = no data.

Sites	Nr. In Fig. 1	Name/nr.	Coordinates site		Depth/thickness/tephra layer	Facies/(sed. Type)	Pollen	14C	Tox.	Refer.
Agro Pontino										
Migliara 44.5	1	44.5	13.0139	41.4484	ca. 100 cm, 2 cm AV	A (3)	–	x	–	Sevink et al. (2011)
Campo inferiore	2	Campo	13.0525	41.4682	ca. 220 cm, 2 cm AV	P/F (1–4)	–	x	–	
Mezzaluna 405	3	405	13.1195	41.4424	ca. 45 cm, 2–3 cm AV	G (2)	x	x	x	Bakels et al. (2015)
Ricci	4	Ricci	13.0374	41.4620	ca. 210 cm, 2–3 cm AV	P/F (1–4)	x	x	–	
Tratturo Canio 455	5	455	12.9937	41.4890	ca. 150 cm, 2–3 cm AV	F (4)	–	x	–	Feiken (2014)
Borgo Hermada 192	6	192	13.1641	41.3209	66 cm, 2 cm AV	G (2)	x	–	x	
Borgo Hermada 362	7	362	13.1575	41.3133	60 cm, 2 cm AV	P (1)	x	x	x	
Borgo Hermada 601	8	601	13.1640	41.3209	60 cm, 2 cm AV	G (2)	x	(x)	–	
Borgo Hermada 602	9	602	13.1701	41.3260	112 cm, 3 cm AV	G (2)	–	x	–	
Cotarda east	10	399	13.1396	41.3997	44 cm, 2 cm AV	A (3)	–	–	x	
Frasso 415	11	415	13.1456	41.3596	106 cm, 3 cm AV	P (1)	–	–	x	
Frasso 500	12	500	13.1462	41.3605	ca. 55 cm, 2 cm AV	P (1)	x	x	–	
Mesa 504	13	504	13.1044	41.3949	44 cm, 2–3 cm AV	A (3)	–	–	x	
Mesa 700	14	700	13.0998	41.4040	46 cm, 2 cm AV	A (3)	–	x	–	
Ricci 372	15	372	13.0270	41.4588	112 cm, 2 cm AV	A (3)	–	–	x	
Fondi										
Femmina Morta 197	16	197	13.3266	41.2968	52 cm, 3 cm AV	P (1)	x	x	x	Doorenbosch & Field (2019)
					66 cm, 2 cm Astr	P (1)	–	x	–	
Tumolillo 1005	17	1005	13.3715	41.2869	88 cm, 2–3 cm AV	P (1)	x	x	–	
					112 cm, 2 cm Astr	P (1)	–	x	–	
Fondi 122	18	122	13.3951	41.3141	81 cm, 2 cm AV	P (1)	x	x	–	
Other sites										
Borgo Hermada 180		180	13.1749	41.3246	AP2	G (2)	–	–	–	
Borgo Hermada 181		181	13.1720	41.3249	AP2	G (2)	–	–	–	
Borgo Hermada 198		198	13.1717	41.3248	AP2	G (2)	–	–	–	

of such plant macro remains and charcoal by soil fauna is well known (Eisenhauer et al., 2009; Forey et al., 2011; Domene, 2016). If by earthworms, it is known to be accompanied by transport of pollen in their excreta (see for instance Van Mourik, 1999). This would likely lead to absence of temporal variability in the pollen record, betraying the homogenizing earthworm activity. The situation is different if such transport was preferential – only plant macro remains - or the transport of pollen was of too limited magnitude to induce a recognizable homogenization of the pollen archive. Preferential downward transport of seeds is for example known from ants (Majer et al., 2008; Robins and Robins, 2011; Kovář et al., 2013). Evidently, such faunal activity will not extend below the mean lowest groundwater level, but short dry spells may have sufficed for some bioturbation to have occurred.

Only site 197 at Femmina Morta shows some evidence of preferential downward transport of plant macro remains. Its palaeoecological record exhibits well defined temporal variations in the composition of the pollen assemblages and macro remains that were identified (see Fig. 5 and Doorenbosch and Field, 2019). However, the ^{14}C ages obtained for plant macro remains are virtually identical, independent of their depth of sampling. Even where taken from below the Astroni layer (indicated as Astr layer in appendix A) the material is slightly younger than the AV layer. At the Tumulillo site this Astr layer was found to date from between 3720 and 3765 B P (c. 2150 cal yr BC, see section 2), The pollen record demonstrates a drier phase with slightly better drainage and lower accumulation rate, following on the deposition of the AV layer (Doorenbosch and Field, 2019). It is this period with better drainage in which the bioturbation may well have taken place, which evidently also would explain the younger age of the plant materials dated. Moreover, in the thin section of the AV layer and adjacent peat layers clear indications exist for such bioturbation in the form of some large biopores (pedotubules, Brewer, 1964), postdating the AV layer (see Fig. 4). In none of the other sections studied one or more of the above discussed indications for bioturbation have been observed, nor are indications for homogenization found in the pollen records.

4.3. Old wood effect ('inbuilt age')

This effect can only be expected for samples that indeed consist of wood, but it is more complex than simply 'old wood' and is now commonly referred to as 'inbuilt age' (see Dee and Bronk Ramsey, 2014). In cases where bark is analysed, outer annual rings of larger wood fragments, or wood in the form of small twigs, a significant 'traditional' old wood effect can be ruled out, such as for the sample from Mezzaluna (see appendix A: GrM-17418) and some wood samples from Campo inferiore (appendix A: Tree trunk, outer 2–5 rings; see also Sevink et al., 2011). Wood samples of uncertain origin (i.e. unknown position within a trunk or larger branch) were excluded during our sampling. In contrast, samples from above the AV layer at Campo inferiore dated by Sevink et al. (2011) were indeed such undefined wood samples (appendix A: GrA-46210 and -32454). They were obtained from a peat layer above the AV layer, which overall was strongly decomposed. Sevink et al. (2011) described that it was only in a small depression that this peat held recognizable plant macro remains (wood) and they assumed that this wood was from a tree postdating the AV layer.

As described by Sevink et al. (2011) and more extensively by Feiken (2014), the many large beams and poles encountered below the AV layer at that site must have been cut down by contemporary Early Bronze Age peoples, who worked trunks and large branches into poles and beams by removing bark, wood and side branches. This happened prior to the deposition of the AV tephra. It cannot be excluded that some trees survived the tephra fall and earlier downcutting of the alder forest, to die and fall on top of the AV layer at a later stage. This would also be an example of the inbuilt age effect and would readily explain the unexpected age of the wood samples from above the AV layer at Campo inferiore.

A rather similar effect may occur in cases where older sediment is eroded and subsequently deposited on top of the AV layer. Such phenomenon might occur when tephra deposition causes a major reduction in biomass and biomass production (see 4.4.2), leaving nearby older sediment exposed to erosion while insufficient 'fresh' biomass is produced to mask the effect of the reworked organic matter on the overall

Table 2
Data on selected samples from below (upper series) and above the AV-layer (lower series). EBA/MBA = Early/Middle Bronze Age. Inbuilt age: x = unsuitable for further analysis because of inbuilt age; ? = possible error because of inbuilt age. Biot. = Bioturbation; x = unsuitable for further analysis because of bioturbation. Hiatus = unsuitable because of hiatus. Strat. Pos.: ? = uncertain origin of material. For facies and sediment type: see Table 1.

Stratigraphic and Contextual Information			Conventional Radiocarbon Age				Characteristics					Sample Error (Years)						
Cores/sections	Name/ number	Description	Lab Ref.	Age (yr BP)	± σ	Sample Material	Facies/sed. Type	Inbuilt age	Biot.	Hiatus	Strat. Pos.	Rate (cm/ cent.)		Mean offset	Absolute range (yrs)		Sample Error	
												Min	Max	μ (cm)	Min	Max	μ (yrs)	± σ
Above AV-tephra layer																		
Agro Pontino																		
Migliara 44.5	44.5	Base layer 4, 1–2 cm above tephra layer	GrA-46203, 46,205	3685	25	Org. Matter	A (3)	x	–	x	–	–	–	–	–	–	–	–
Campo inferiore	Campo	Above tephra layer	GrN-32454	3635	40	Wood	P/F (1–4)	x	–	–	–	–	–	–	–	–	–	–
		Above tephra layer	GrA-46210	3610	30	Wood		x	–	–	–	–	–	–	–	–	–	–
Ricci	Ricci	Wood in EBA II or MBA I vessel	GrA-51750	3445	35	Wood	P/F (1–4)	–	–	–	?	–	–	–	–	–	–	–
Tratturo Canio	455	layer 5001 (c. 5–10 cm above tephra layer)	GrA-44910	3495	45	Charcoal	F (4)	–	–	–	–	–	–	–	–	–	–	–
Frasso 500	500	Above tephra layer (within 2 cm)	GrM-17223	3505	25	Wood	P (1)	–	–	–	–	6	12	1.0	8	17	13	2
		Above tephra layer (within 2 cm)	GrM-17840	3365	40	Charred seeds		–	–	–	?	–	–	–	–	–	–	–
Mesa	700	Black peat/clay, 0–1 cm above tephra layer	GrM-17888	3085	35	Org. Matter	A (3)	–	–	x	–	–	–	–	–	–	–	–
Borgo Ermada 362	362	BE 362 57–58 cm, tephra at 60–62 cm	GrM-17231	3415	25	Seeds	P (1)	–	–	–	–	6	12	2.5	21	42	31	5
Fondi																		
Femmina morta	197	FM 7 42–50 cm, above tephra layer (52–54 cm)	GrA-67046	3380	35	Wood	P (1)	–	x	–	–	–	–	–	–	–	–	–
Fondi 122	122	Fondi 122A 79-80 cm, above tephra (81-83 cm)	GrM-17887	3500	50	Charcoal	P	-	-	-	-	6	12	1.5	13	25	19	3
Below AV-tephra layer																		
Agro Pontino																		
Migliara 44.5	44.5	Top layer 2, 1–2 cm below tephra layer	GrA-46200, 46,201	3565	25	Org. Matter	A (3)	–	–	–	–	3	6	1.5	25	50	38	6
Campo inferiore	Campo	c. 6 cm below tephra layer	GrA-45134, 45,265, 45,266	3585	20	Tree leaves	P/F (1–4)	–	–	–	–	6	12	6.0	50	100	75	13
Ricci	Ricci	7 cm below AV-layer	GrA-56630	3600	45	Seed and catkin	P/F (1–4)	–	–	–	–	?	?	7.0	–	–	–	–
Mezzaluna	405	Tree trunk from below gyttja (10 cm below AV)	GrM-17418	3735	25	Outer tree rings	G (2)	–	–	–	–	15	20	10.0	50	67	58	4
Frasso 500	500	Below tephra layer (within 2 cm)	GrM-17225	3530	25	Twig	P (1)	–	–	–	–	6	12	1.0	8	17	13	2
		idem	GrM-17226	3610	25	Charred seeds		?	–	–	?	–	–	–	–	–	–	–
Mesa	700	Black peat/clay, 0–3 cm below tephra layer (C2)	GrM-17495	3590	25	Org. Matter	A (3)	–	–	–	–	3	6	1.5	25	50	38	6
Borgo Ermada 602	602	121–127 cm: tephra at 112–115 cm	GrM-17907	3570	25	Seeds	G (2)	–	–	–	–	15	20	9.0	45	60	53	4
Fondi																		
Femmina morta	197	FM 5 54–56 cm: Below tephra layer (52–54 cm)	GrM-16626	3495	25	Leaf fragment	P (1)	–	x	–	–	?	?	2.0	–	–	–	–
		FM 5 54–56 cm: Below tephra layer (52–54 cm)	GrM-18970	3488	25	Seeds		–	x	–	–	?	?	2.0	–	–	–	–
Tumolillo	1005	Tumolillo 90–91 cm: Below tephra (88–90 cm)	GrM-16620	3550	30	Seeds	P (1)	–	–	–	–	6	12	0.5	4	8	6	1
		Tumolillo 90–91 cm: Below tephra (88–90 cm)	GrM-17417	3570	25	Charcoal		–	–	–	–	6	12	0.5	4	8	6	1
Fondi 122	122	Fondi 122 A 83–84 cm: Below tephra (81–83 cm)	GrM-17227	3555	25	Charcoal	P (1)	–	–	–	–	6	12	0.5	4	8	6	1
		Fondi 122 A 85–86 cm: Below tephra (81–83 cm)	GrM-17228	3580	25	Charcoal		–	–	–	–	6	12	2.5	21	42	31	5

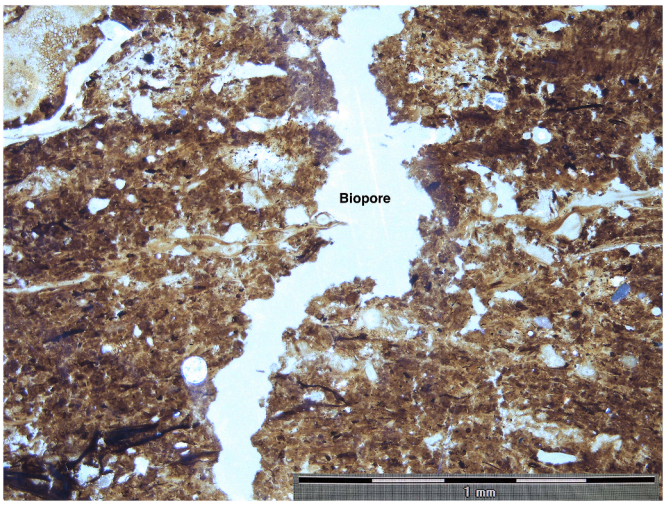

Fig. 4. Thin section of the AV-tephra layer at Femmina Morta with distinct pedotubules (indicated as 'biopore').

^{14}C age of the accumulated sediment. Such an effect may have occurred in the anoxic pyritic environment at Migliara 44,5 and explain the aberrant high age of the black organic clay samples from above the AV layer at that site.

4.4. Sampling error

As described previously, to obviate hard water effects, macro remains of plants known to take their carbon dioxide from the atmosphere were selected for ^{14}C dating wherever possible, but concentrations of such remains were low, implying that often sediment slices several centimetres thick were needed to retrieve sufficient material. In cases where the accumulation rate was low this may induce a significant 'sampling error'. Various strands of evidence are relevant here, including a) potential sampling errors based on sample size and estimated accumulation rate; b) indications for post-tephra accumulation rates from the palaeoecological data; and c) potential toxic impacts of tephra. These various aspects are discussed separately.

4.4.1. Accumulation rates

Mean accumulation rates, calculated for the sediment sequences studied, are presented in Table 3A and testify to the very low mean rates for the deposits in both coastal areas. However, these mean values may be biased by very low accumulation rates from the Early Iron Age onwards (ca. 1000 BCE), post-AV accumulation rates having been much higher initially and strongly slowing down later on. This scenario seems very realistic, given the outcomes of numerous studies on early land use in the Agro Pontino (Van Joolen, 2003; Feiken, 2014; Attema, 2017; De Haas, 2011, 2017). These studies showed that though fluvio-colluvial sediments (indicated as 'young colluvial deposits' in Fig. 3) are rather widespread, which suggests a massive supply of eroded soil material that was mainly transported by canal-like streams, the accumulation rate was very much lower outside the locations where this sediment was deposited. In these areas, rates have been very low since at least the Early Roman times. The major argument for such lack of significant accumulation is that remains of Early Roman and later land use are found in topsoils of the Holocene Terracina deposits all over the interior Agro Pontino basin (Feiken, 2014; Attema, 2017; De Haas, 2017). Moreover, the Early Roman artefacts are frequently found at the current land surface, testifying to very low accumulation rates outside the fluvio-colluvial areas for this later period.

Higher accumulation rates and thus lower sampling errors are found for the cores holding two tephra layers (Table 3B). The age of the AP2 and Astroni 6 tephra layers is not truly precisely known (see section 2 above) but can be set at c. Two centuries later and earlier, respectively. Rates calculated for such intervals are much closer to the values from the literature for cores from central Mediterranean sedimentary complexes (Table 4) and thus seem much more reliable and for that reason have been used to estimate the 'sampling error'. The five cores for which we could calculate these rates represent specific sedimentary environments – types 1 and 2 – for which toxic impacts of the tephra are expected to be limited or even absent (see 4.4.2).

4.4.2. Potential toxic impact of tephra

As discussed before, four types of sedimentary environments were distinguished each of which has its characteristic geochemical conditions. In a sulphidic anoxic environment (type 3), for example, many heavy metals are immobilized in the form of highly insoluble metal sulphides (e.g. Krauskopf, 1967; McBride, 1994; Sundelin and Eriksson, 2001). Thus, if present in the tephra, these heavy metals may show up as spikes, whereas in the highly calcareous lacustrine environment in which type 2 sediments were formed, fluorine (F) will be immobilized in the form of CaF_2 (e.g. Garand and Mucci, 2004). Spikes of elements that are known to occur in the Vesuvian ejecta (e.g. Signorelli et al., 1999; Balcone-Boissard et al., 2012) thus can be explained as resulting from tephra deposition. Evidently, if immobilized, these elements are very unlikely to have had a toxic impact, but in contemporary environments in which such immobilization did not occur, the opposite may be true. Pb for example will be immobilized in an anoxic sulphidic environment, but because of its mobility in well aerated aquatic environments may have reached toxic levels in the latter. On the other hand, if fallen into well aerated waters which were rapidly refreshed, this dilution is very likely to have prevented toxic levels to be reached.

Table 5 shows that overall concentrations of specific elements in the sediments sampled are quite variable. For example, Zn reaches high levels in the Mezzaluna section but is low at other sites such as Mesa. We did not find distinct spikes of heavy metals that can be linked to the AV layer and are also commensurate with specific sediment types. Zn seemingly exhibited such spike in the Mezzaluna core, but in none of the other cores. The only clear spike is the F-spike found at both Mezzaluna 405 and Borgo Hermada 601. These are both from gyttja deposits with intercalated tephra layer. Since F will remain mobile in aquatic environments with low Ca concentrations, we refrained from extensive F-analyses of such sediment types (types 1, 3, 4) and assumed that F-spikes would not be encountered. This is corroborated by the analyses for Borgo Hermada 362 (type 1 sediment), in which F-values are slightly higher, but no distinct spike occurs.

The data for the Mezzaluna 405 and Borgo Hermada 601 sections thus strongly suggests that the tephra contained F, which was most probably immobilized in the highly calcareous lacustrine environment in the form of CaF_2. F-concentrations in this tephra were in the order of 2 g/kg, given the concentration of tephra in the layers analysed, which is defined as the fraction >63 μm (see Table 5). These F-concentrations are in the same order as reported critical health values for fluorine (e.g. Cronin et al., 2003; Weinstein and Davison 2004; Hansell et al., 2006; Petrone et al., 2011) and in line with its reported values in Vesuvian ejecta (Signorelli et al., 1999; Balcone-Boissard et al., 2012). In fact, Cubellis et al. (2016) reported even higher concentrations for the 1944 Vesuvius eruption (up to 0.5 wt percentage - 5 g/kg) and described the serious environmental health problems resulting from these ashes. That the F-levels from earlier Vesuvian eruptions also led to serious human health problems was demonstrated by Petrone et al. (2011).

To what extent this F may have affected the vegetation is less clear, since available studies on the impact of F (e.g. Grattan and Pyatt, 1994; Koblar et al., 2011; Kumar et al., 2017; Banerjee and Roychoudhury, 2019) point to diverse and species dependent impacts and results published cannot readily be applied to wetland ecosystems. Moreover, studies on the impact of tephra on wetland ecosystems rarely pay attention to the impact of F (e.g. Hotes et al., 2004; Ayris and Delmelle, 2012). Nevertheless, it is clear that fluorine is indeed a biohazardous

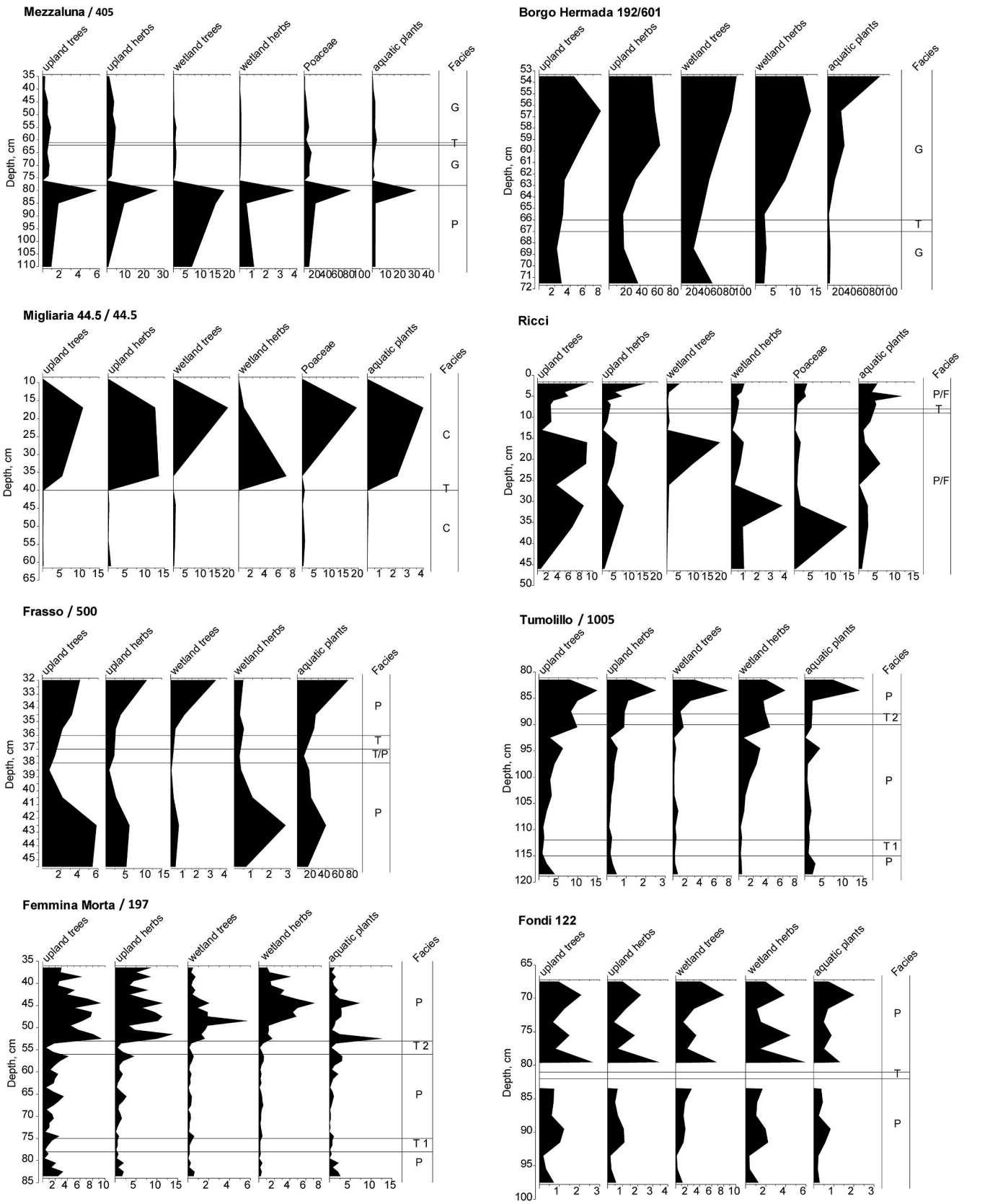

Fig. 5. Pollen concentration diagrams from the sections studied. Indications of facies following Table 4; T = AV tephra.; T 2 = Astroni tephra. Concentration in numbers x 10^4 per 1 cm^3.

Table 3
A: Mean accumulation rates for the post-AV sediment in the sections studied, based on depth in cm of the AV-layer below the land surface (in the absence of a colluvia-alluvial cover) or below the base of the colluvio-alluvial cover. Estimated age of burial is based on ^{14}C dating of the base of the colluvio-alluvial cover (see Van Joolen, 2003; Feiken, 2014).B: Accumulation rate for the inter-tephra sediment (between Astroni and AV-layer, and between AP2 and AV-Layer).

A: mean accumulation rates

Site	Name/nr.	Tephra layer	Facies	Pollen	Thickness in cm	Age	Rate cm/cent	Refer/comments.
Agro Pontino								
Migliara 44.5	*44.5*	*c.* 100 cm, 2 cm AV	*A*		*50*	*1500*	*3*	Sevink et al., (2011)/Feiken (2014)
Campo inferiore	*Campo*	*c.* 220 cm, 2 cm AV	*F*		*50–60*	*c. 1500*	*3–4*	Sevink et al., (2011)/Feiken (2014)
Mezzaluna	*405*	*c.* 45 cm, *2*–3 cm AV	*G/P*	*x*	*45*	*c. 4000*	*c. 1*	Bakels et al. (2015)
Ricci	*Ricci*	*c.* 210 cm, *2*–3 cm AV	*F*	*x*	*60*	*c.1400*	*c. 2.5*	Bakels et al. (2015)
Tratturo Canio	*455*	*c.* 150 cm, *2*–3 cm AV	*F*		*n.d.*	*n.d.*	*n.r.*	Feiken (2014)*: archeol.site*
Frasso 415 core	415	106 cm, 3 cm AV	P		n.d.	n.d.	n.r.	
Frasso 500 pit	500	c. 55 cm, 2 cm AV	P	x	55	4000	c. 1	
Mesa (pit)	504	46 cm, 2 cm AV	A		46	4000	c. 1	
Mesa core	700	44 cm, 2–3 cm AV	A		44	4000	c. 1	
Borgo Hermada 362	362	60 cm, 2 cm AV	P	x	60	4000	c. 1.5	
Borgo Hermada 601-1	601	60 cm, 2 cm AV	G		60	4000	c. 1.5	
Borgo Hermada 602-1	602	112 cm, 3 cm AV	G		112	4000	c. 3	
Ricci 372	372	105 cm, 2 cm AV	A		45	1500	c. 3	
La Cotarda East 399	399	44 cm, 2 cm AV	A		44	4000	c. 1	
Fondi								
Femmina morta	197	50 cm, 3 cm AV	P	x	50	4000	c. 1	Doorenbosch & Field (2019)
Tumolillo	1005	88 cm, 2–3 cm AV	P	x	23	3800	c. 1	
Fondi 122	122	81 cm, 2 cm AV	P	x	42	2000	c. 2	

B: accumulation rates based on tephra ages

Site	Name/nr	Upper tephra layer/cm	Facies	Rate cm/cent
Borgo Hermada	181	AP2 - 39 cm	G	20
Borgo Hermada	198	AP2 - 33 cm	G	16.5
		Lower tephra layer/cm		
Femmina morta	197	Astroni 12 cm	P	6
Tumolillo	1005	Astroni 22 cm	P	11

Table 4
Overview of data on accumulation rates and sampling for published cores from the Tyrrhenian coastal area of central Italy. For Facies, see Table 1.

Site	Environment	Accumulation rate in 100 years	Sections	Sample thickness	Source
Gulf of Gaeta	Shelf	10 cm	2 cores (composite)	86 samples over 480 cm for pollen, no further relevant data (no 14C)	Di Rita et al., 2018/Margaritelli et al. (2016)
Garigliano	Coastal lagoon	6–8 cm	several cores	no information	Bellotti et al. (2016)
Maccarese	Tiber delta/ lagoon	8 cm	1 core	probably 5 cm sample thickness but no precise information	Jouannic et al. (2013)
Mezzano	Crater lake	c. 15 cm	3 cores	bulk samples, 3 cm	Ramrath et al. (1999)
Accesa	Karstic lake	c. 15 cm	several cores	1–2 cm	Magny et al. (2007)
Ombrone	River delta	8–10 cm	1 core	2–4 cm	Biserni and Van Geel, 2005
Albano	Crater lake	c. 10 cm	several cores	no information	Ariztegui et al. (2001).

agent. That the tephra deposition may indeed have led to a major reduction in biomass production is strongly suggested by the results for Mesa, where material from immediately above the AV layer returned an age of 3085 years BP. A standstill in the accumulation of material evidently may lead to significantly younger ^{14}C ages and cause a typical 'sampling error'.

In summary, fluorine concentrations in the AV tephra will have been at least in the order of 2 g/kg. If deposited in a semi-aquatic environment in which dilution was restricted, this may well have led to a toxic concentration of fluorine negatively affecting the vegetation, such as in the very tranquil anoxic and sulphidic environments described as type 3. If directly diluted or immobilized in an environment that was oversaturated relative to calcium carbonate, a toxic impact is far less likely to have occurred (types 1, 2 and 4).

4.4.3. Palaeoecological data

The first question is whether regrowth of vegetation after tephra deposition was instantaneous and the accumulation of organic material, calcareous gyttja or clastic sediment was a rather continuous process or was more or less seriously interrupted by the tephra deposition. Indicators for such impact may be a) a sudden increase of the pollen concentration of plant species growing outside the wetlands where the deposits were formed (upland plants) and b) a sudden decline in the amount of pollen released by peat-forming plants (wetland plants).

In Fig. 5 data are presented on the pollen concentrations in the various sections studied. Trees and shrubs are depicted separately from herbs in order to allow the consideration of a possible influence of deforestation around the basins and within their margins which might affect conclusions. In some diagrams the original authors set the Poaceae (grasses) apart because they might represent peat-forming reeds on the one hand, but upland grasses at the other. The clearest example of absence of any effect of tephra deposition is the calcareous gyttja of Mezzaluna (type 2), but also the gyttja of Borgo Hermada 192/601 (type 2) and the peat of Ricci (type 2–4) show no immediate reaction after the AV event. They markedly differ from the pattern in the section from Migliara 44,5, with type 3 sediment, in which a massive increase is observed. Trends in type 1 sediment are rather variable. In the Femmina Morta and Fondi 122 sections the effect is considerable. In Tumolillo 2 change apparently set in before the deposition of the volcanic ash, whilst the Frasso 500 section provides no clues at all. It is striking that in the

Table 5
Chemical composition of tephra and adjacent strata. For sediment type symbols, see Table 1. AV-tephra layer is indicated in grey.

Profile + sediment type	Depth in cm	Zn	Pb	Hg	Cr	V	Cu	Sr	F	% >63 um
		(mg/kg)							(g/kg)	
Mezzaluna 405 (G)	39–41	1623	27	67	x	x	15	545	0.4	
	41–43	1925	34	68	x	x	18	509	0.4	
	43–45	2373	39	96	x	x	25	372	0.9	38
	45–47	1249	25	72	x	x	17	468	0.4	
	47–49	1464	28	72	x	x	16	459	0.3	
Mesa 504 (A)	40–42	42	45	307	123	150	104	307	n.d.	
	42–44	41	31	252	115	140	109	258	0.3	
	44–45	53	46	263	111	164	126	246	n.d.	3
	45–46.5	51	43	228	80	162	108	255	n.d.	
	46.5–48	49	43	187	71	118	112	233	n.d.	
Frasso 415 (P)	101–104	81	42	132	92	188	54	189	n.d.	
	104–106	75	x	118	86	176	51	188	n.d.	
	106–109	51	80	99	40	98	33	197	n.d.	16
	109–112	72	x	129	81	144	48	169	n.d.	
	112–115	89	x	110	98	128	39	144	n.d.	
	115–117	90	x	103	100	132	40	150	n.d.	
La Cortarda 399 (A)	40–42	81	39	133	105	190	52	153	n.d.	
	42–44	76	41	135	104	187	51	147	n.d.	
	44–46	78	47	106	82	167	37	173	n.d.	7
	46–48	57	x	103	86	119	33	109	n.d.	
	48–50	49	57	114	87	112	28	107	n.d.	
Ricci 372 (A)	108–110	104	51	137	118	221	75	171	n.d.	
	110–112	105	60	141	114	226	74	176	0.4	
	112–114	99	51	138	132	181	63	199	n.d.	18
	114–116	106	50	126	116	201	72	172	n.d.	
	116–118	110	43	129	125	194	72	167	n.d.	
Borgo Hermada 362 (P)	56–58	1510	31	232	69	63	47	150	0.2	
	58–60	1214	32	194	59	58	44	157	0.2	
	60–62	731	34	135	44	56	41	231	0.4	33
	62–64	803	39	145	42	56	43	279	0.4	
	64–66	645	39	166	61	62	41	449	0.2	
Femmina Morta 197 (P)	46–48	28	36	94	10	55	44	193	n.d.	
	48–50	41	49	98	8	69	49	228	n.d.	
	50–52	4	39	81	5	68	46	164	n.d.	43
	52–54	x	40	84	5	62	43	138	n.d.	
	54–56	x	41	82	2	60	35	220	n.d.	
Borgo Hermada 601*(G)	58–60	19	6	x	20	26	20	707	0.5	
	60–62	28	10	x	20	38	20	713	0.7	
	62–65	41	16	x	30	56	20	680	0.7	n.d.
	64–66	39	10	x	40	54	20	719	0.3	
	66–68	39	12	x	50	53	20	908	0.2	
	68–70	41	9	x	50	56	20	875	0.3	
	70–72	44	14	x	50	62	20	841	0.2	
	72–74	48	13	x	60	67	20	937	0.3	
* Actlab	Det. Limit.	1 (ICP)	5 (MS)	1 (ICP)	20 (MS)	2 (ICP)	10 (MS)	2 (ICP)	0,1 (ISE)	

two sites, which display a possible adverse effect on peat accumulation, the kinds of vegetation responsible for peat formation, wetland herbs and wetland trees, do not behave different from the others (Fondi 122) or even lag behind (Femmina Morta).

Overall, the data suggest that the vegetation and accumulation of calcareous gyttja and peat in a type 2 environment were not affected by the toxic tephra, whereas the accumulation of sediments in a type 3 environment was lowered to a considerable degree. The situation in type 1 environments proved to be ambiguous. Eventually, slight differences in water depth and associated water flow may have existed, which explain these differences within the latter type of environment.

4.4.4. *Estimating sampling errors*

Estimations of the accumulation rates for the various types of sedimentary environments can be based on the data presented in Tables 3B and 4 and formed the basis for our distinction of three ranges for the various sedimentary environments: 3–6 cm/century for type 3, 6–12 cm/century for type 1, and 15–20 cm/century for type 2. These values have been used to calculate the sampling error for specific samples, based on accumulation rate and mean sampling depth. Values thus obtained are presented in Table 2 for samples that are not deemed to be unsuitable for other reasons (inbuilt age, bioturbation, hiatus or uncertain stratigraphic position) and are calculated for minimum and maximum accumulation rates (listed as 'Rate', with minimum and maximum values). The uncertainty linked to the thickness of the sampled layer, which is not taken into account in the calculated 'absolute range', is of minor importance, since it does not affect the error (μ) itself, but rather the significance (±σ) of this error. For Frasso 500 GrM 17,223, for example, the 'absolute range' given in Table 2 is 8–17 years with an error of 13 years, whereas if including the uncertainty linked to the thickness of the sample (2 cm) this range would become 0–33 years. For samples that are from layers that are 1 cm thick the inclusion of the

uncertainty linked to thickness of the layer sampled leads to even smaller differences, such as for Fondi 122 GrN 17,227 (range 4–8 years versus range 0–16 years). Evidently, in case that accumulation rates are low and thicker layers are sampled, larger and more relevant differences will occur between these calculated sample errors and in that case have to be accounted for. For a full discussion of this aspect, reference is made to appendix B.

Characteristics that in our set of sites restrict the use of ^{14}C dates for a Bayesian analysis include inbuilt age, bioturbation, hiatus, and uncertain stratigraphic position. Hiatuses are typical for post-AV sections in type 3 sedimentary environments, where clear indications exist for a toxic impact of tephra deposition and associated major reduction of accumulation rates, based on the pollen density profiles. These ecosystems are evidently fragile (Bagarinao, 1992) and the vegetation may need considerable time for recovery, if impacted by toxic tephra. The pollen concentration graphs indicate that accumulation rates in type 1 and 2 environments were not or only marginally affected by tephra deposition. Unfortunately, our type 2 environments are fundamentally unsuitable for ^{14}C dating for other reasons (no suitable plant macro remains). This is exemplified by the Mezzaluna site, where such plant macro remains are indeed absent in the calcareous gyttja and a relatively large error is found for the wood sample from below this gyttja, which hampers the use of this date. Sediment accumulation rates for the fluvio-deltaic sites (type 4 environment) are highly uncertain and sequences are likely to have hiatuses. The overall conclusion is that for samples from type 1 environments, taken as thin layers from directly above and below the AV layer the sampling error is of minor relevance only and that such samples are ideally suitable for ^{14}C dating and constraining the age of the AV layer.

Table 2 thus shows the offset linked to the sampling error for those samples for which such offset can be reliably calculated. The mean offset in years (calculated from the mean distance and mean sedimentation rate) is a tentative measure for the age of the AV layer relative to the calibrated age of the sample concerned. Offsets for the sites Frasso (500), Tumolillo (1005), and Fondi (122) are small, while those for Campo inferiore (Campo), Mezzaluna and Borgo Ermada 601 are quite large.

4.5. Configuration of the bayesian models

Two different modelling approaches were applied to the ^{14}C data traversing the AV layer in an attempt to bring together all the evidence and refine the eruption date. All analyses were conducted in the program OxCal (version 4.3, Bronk Ramsey, 1995; 2017). For details reference is made to Appendices B and C.

4.5.1. Model 1

The first approach consisted of a simple two-Phase Sequence with one Phase for the dates obtained above the tephra and one for the dates below the tephra. This is a legitimate configuration for such an analysis because, although the samples come from disparate sites, in chronological terms they are clearly distinguishable by this one criterion. Further, by placing the dates in Phases no relative ordering information between the samples is assumed and the underlying premise is that within each Phase the results are uniformly distributed over a period of time determined by the program itself. This is advantageous for our study because it is clear some results are significantly more offset than others from the true date of the eruption. Furthermore, in order to ensure the final outputs were not biased by a small number of particularly outlying data, use was made of OxCal's Outlier functionality. This feature automatically filters out individual results that are inconsistent with the data set as a whole. In Model 1, every ^{14}C date was given an equal (5%) prior probability of being an outlier, and during the iterative process the algorithm downweighed the contribution of the most wayward dates to the final outputs. All 25 ^{14}C dates listed in Table 2 were included in the model. A comparative model (S1) is given in appendix C which, instead of outlier analysis, employed the removal of the dates with the lowest Agreement Indices until the overall model reached 60% Agreement. The OxCal codes for both Model 1 and S1 are given in appendix C.

4.5.2. Model 2

A second approach was taken where closer attention was paid to the sampling error discussed in detail in this paper. In practice, this involved using the estimated sedimentation rates to correct for the sampling error inherent in each result. As shown, not all of the dates in Table 2 were eligible for this analysis. It could only be applied to those from sites where reliable and uninterrupted sedimentary rate information was available. In all, thirteen dates met these criteria. Using OxCal, the ten eligible dates before the eruption were shifted to younger ages and three dates after the eruption shifted to older ages. The shift was applied using a simple Normal distribution centred on the mean sedimentary rate, with a 2-sigma range that extended from the minimum to the maximum absolute sampling error. To clarify, a sample centred 2 cm below the tephra at a site with a sedimentation rate of ranging from 5 (min.) to 10 (max.) cm/century required a shift of 20 (min.) to 40 (max.) years. In such a case, the calibrated date was shifted by a factor of 30 ± 5 years (1-sigma). Finally, all the adjusted dates were averaged by reusing them as prior probabilities in a bounded Phase containing a Sum function (see Dee et al., 2014). For this last step, each adjusted date was also given a 5% prior probability of being an outlier, to ensure no extreme results biased the final average. The configuration adopted for Model 2 is a simplification, given the notorious irregularity of calibrated ^{14}C dates. However, as the shifts were only of the order of decades and very minor in comparison to the breadth of the unmodelled calibrations themselves, it was considered acceptable for exploratory purposes. A comparative model (S2) is given in the appendix which, instead of outlier analysis for the final step, employed the removal of the dates with the lowest Agreement Indices until the overall model reached 60% Agreement. The OxCal codes for both Model 2 and S2 are given in appendix C.

4.5.3. Outputs of bayesian models

Fig. 6 shows the position of the Avellino tephra in relation to all the individual dates included in Model 1. The model identified three dates as being extreme outliers: one in the pre-eruption group (GrM-17418, Mezzaluna) and two in the post-eruption group (GrA-46203, 46,205, Migliara 44.5; GrM-17888, Mesa 700). These were essentially eliminated from the analysis. The model also downweighed the contribution of four other dates (GrA-46210, Campo; GrN-32454, Campo; GrM-18970, Femmina Morta, GrM-16626, Femmina Morta) as they were only deemed partially in agreement with the sequence as a whole. The date for the Avellino eruption from Model 1 is somewhat bimodal in nature and extends from 1934 to 1841 cal BC at 95% probability. The alternative model S1 generated a congruent date of 1910–1810 cal BC at 95% probability, producing a broader range than using outlier analysis.

Fig. 7 shows the dates used for Model 2 before (7a) and after (7 b) their shifts to account for sampling error. As is apparent, the adjustments had a very limited effect on the absolute position of the dates. Nonetheless, the adjusted dates should in theory overlie the eruption date, and thus can be averaged to estimate the date of the eruption (Fig. 8). This smaller data set was internally very consistent, and only sample (GrM-17418, Mezzaluna) was regarded as an extreme outlier. The modelled date for the Avellino eruption obtained by Model 2 was 1909–1868 cal BC at 95% probability. The alternative model S2 generated an almost identical date of 1907–1869 cal BC at 95% probability.

For comparative purposes, the modelled dates for the eruption from Model 1 and from Model 2 are shown alongside each other in Table 6 and in Fig. 9. The overwhelming picture is that the results obtained from the two different methods are highly compatible with each other and, notwithstanding all of the preceding discussions about the challenges involved in dating this tephra layer, they represent a credible science-based date for the eruption.

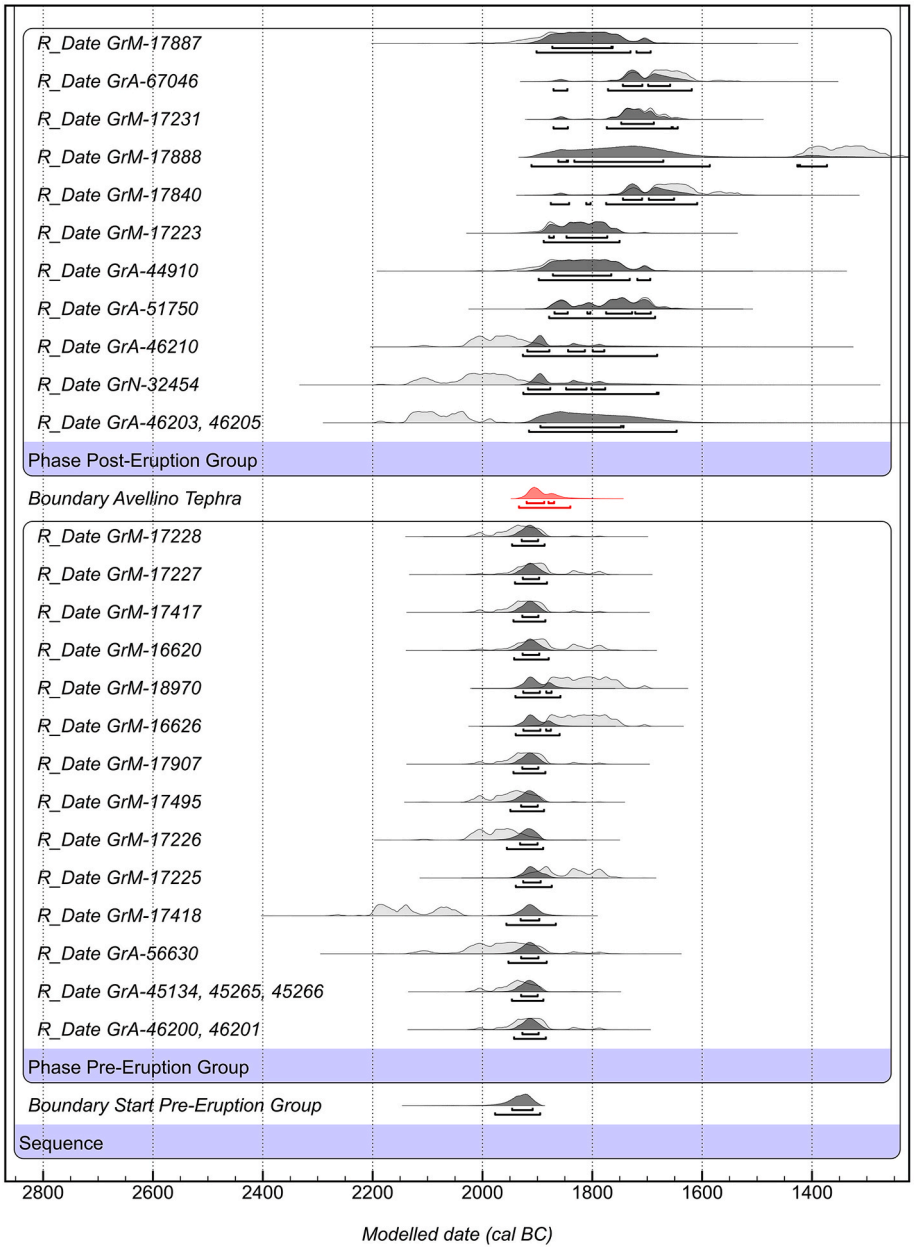

Fig. 6. The outputs from Model 1. The modelled posterior distributions (dark grey) overlie the prior probabilities (light grey). The transitional Boundary marking the Avellino Eruption is shown in red. In each case, the 68% and 95% probability ranges are indicated by the square brackets beneath the modelled estimates. (For interpretation of the references to colour in this figure legend, the reader is referred to the Web version of this article.)

5. General discussion and conclusions

Our study set out to identify factors that might complicate the ^{14}C dating of materials from above the AV layer, paying particular attention to the causes for the wide range in dates obtained. Apart from well-known factors such as the old wood/inbuilt age effect and bioturbation, we looked closer into the sampling error connected with dating plant macro remains from layers that formed in environments with low accumulation rates. The resulting sampling error can be assessed by combining the accumulation rate and thickness of the layer sampled. Particularly in environments with low sedimentation rates (6–8 cm/century or lower) and with sediment holding a low percentage of suitable plant macro remains (>2 cm thick layers sampled), the uncertainty of ^{14}C dates for such materials rapidly increases (see also Appendix B). This rendered these dates less suitable for reliable and precise assessment of the absolute age of the intercalated tephra layer.

The chemical analyses and pollen concentration curves together strongly suggest that the AV tephra held toxic concentrations of F and that its deposition in stagnant anoxic shallow aquatic to marshy environments induced a serious reduction of the sediment accumulation rate, most probably as a result of a reduced biomass/necromass production by the vegetation. Such a toxic impact was rather surprising and not reported earlier for distal areas, even though comparable toxic impacts were well known for proximal Vesuvian areas. Remarkably, it has also not been mentioned as a relevant phenomenon in studies of sites with the AV tephra from such proximal areas and may well have been overlooked. Far more optimal for constraining the age of the AV layer are samples from oxic aquatic to marshy environments in which peat to peaty clays accumulated, where this presumed toxic impact played an at most subordinate role. In these settings, accumulation rates were higher, as were contents of suitable plant macro remains, and thus sampling errors are lower, increasing the statistical reliability of the ages

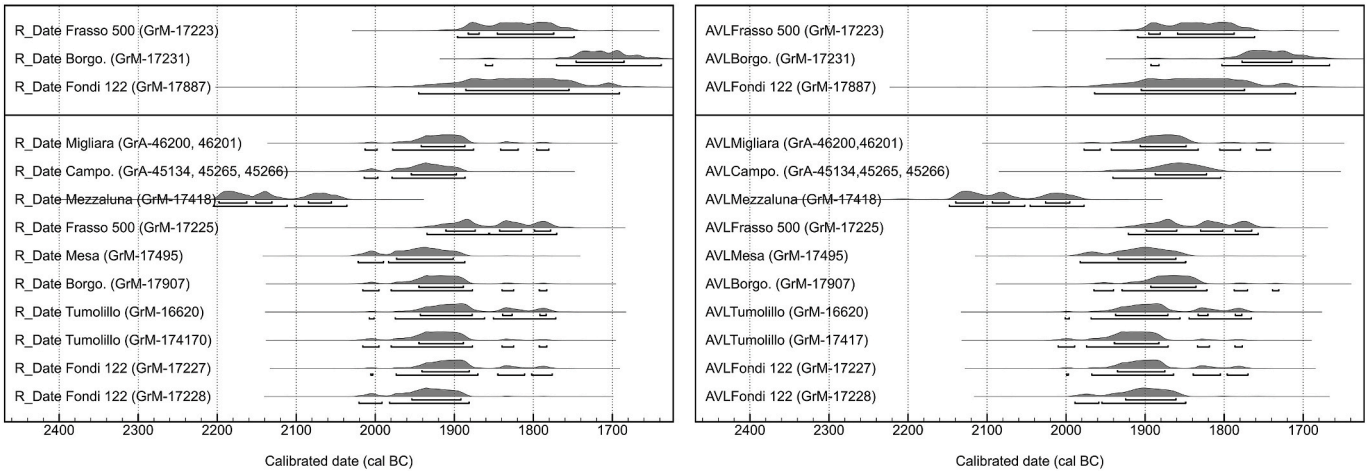

Fig. 7. The calibrated dates utilized for Model 2 before (a) and after (b) the adjustments for sampling error.

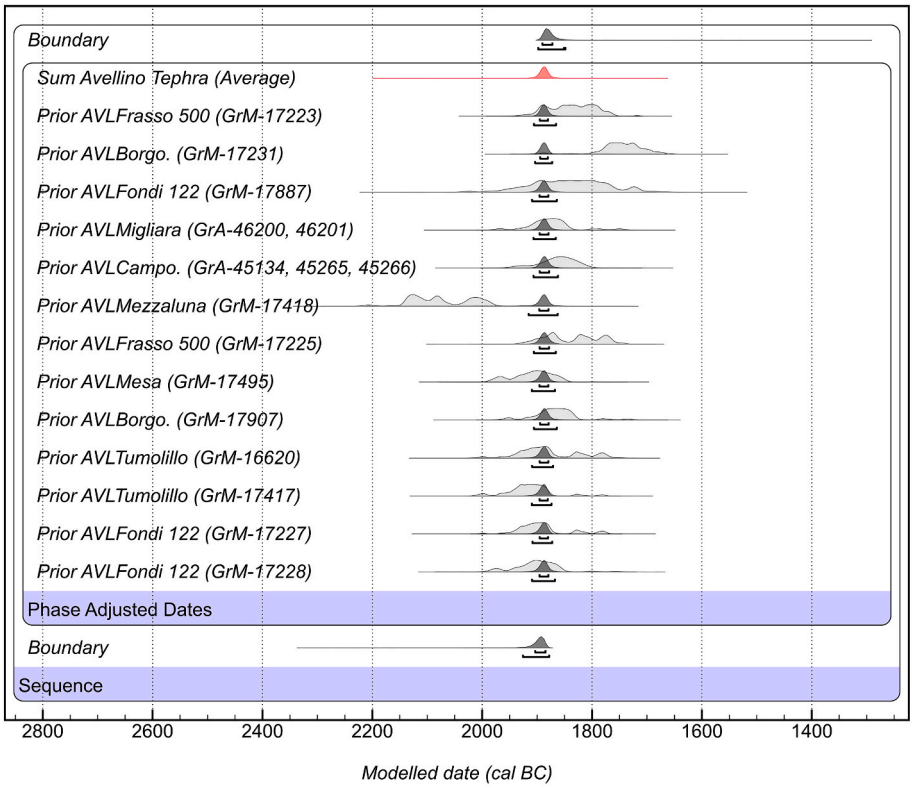

Fig. 8. The averaged date for the Avellino Eruption from Model 2 based on all of the dates adjusted for sampling error.

Table 6
The 68% and 95% probability ranges for the Avellino eruption obtained from Models 1 and 2.

Model	Modelled Date for Avellino Eruption (Year cal BC)			
	From (68%)	To (68%)	From (95%)	To (95%)
1	1920	1870	1934	1841
2	1896	1880	1909	1868

obtained.

Interestingly, samples that in the Bayesian model for the whole dataset (model 1) were discriminated as being 'extreme outliers' or 'partially in agreement with the sequence as a whole' are identical to the samples that based on the factors discussed above (bioturbation, inbuilt age, and sampling error) were considered as suboptimal (see Table 2). This lends further weight to the outcome of model 2, which is based on the Bayesian analysis of the more limited set of samples and includes corrections for the sampling error. This set dominantly concerns samples from type 1 sediment with thicknesses of layers sampled of 2 cm or less, and thus with a small sampling error.

The current results provide a clear explanation for the discrepancy between the earlier published date for the AV layer – 2010–1958 cal BC, 1 σ (Sevink et al., 2011) - and the date established by model 2–1909–1868 cal BC, 1 σ. This earlier dating was based on results that now can be deemed biased by a large sampling error and/or inbuilt age, in combination with a small set of dates, which by statistical coincidence resulted in an age of the AV layer that was interpreted as robust. That

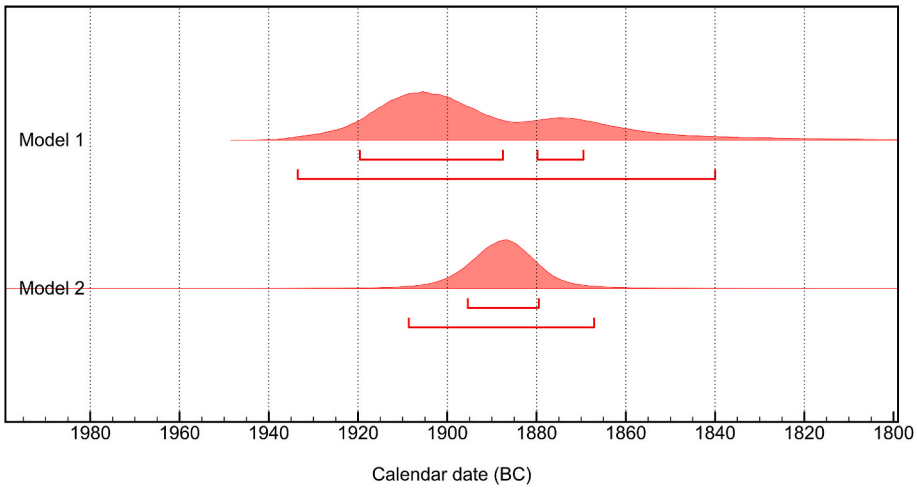

Fig. 9. Comparison of the modelled dates for the Avellino Eruption obtained by Model 1 and Model 2.

this was indeed statistical coincidence is clear from the analysis of the much larger data set that is discussed in this paper.

Our results stress the need to base truly robust dating of distal tephra layers, intercalated in lowland sedimentary sequences, on a critical evaluation of large sets of dates, accounting for potential effects of bioturbation, inbuilt age, and sampling error. By doing so, we now can solve the controversy over the age of the AV layer that resulted from our earlier dating (2011). Our current estimated age is remarkably congruent with the age obtained by Alessandri (2019: 1929–1858 cal BC, 1 σ) and earlier by e.g. Passariello (2009: 1935–1880 cal BC, 1 σ) and Jung (2017: 1908 ± 12 cal BC, with a probability of p = 86%).

More general implications of our research are that ages of distal tephra layers from lowland sedimentary archives in the Mediterranean, if based on a limited set of ^{14}C dates and not supported by a thorough analysis of the potential sampling error, are deemed to remain unreliable. Such analysis should focus on changes in sediment accumulation rates following upon the deposition of tephra, which can be assessed by scrutiny of pollen density profiles across sections containing tephra layers. Our results also suggest that particularly in archives that are more proximal and contain more massive tephra layers, toxic impacts may play an important role and may have led to significant post-depositional hiatuses hampering reliable and precise ^{14}C based assessments of the age of these tephra.

Declaration of competing interest

The authors declare that they have no known competing financial interests or personal relationships that could have appeared to influence the work reported in this paper.

Acknowledgements

We sincerely acknowledge the efforts by many people in both the field and laboratory, particularly the other members of the Avellino project staff: Wouter van Gorp and Luca Alessandri (Groningen University), and Marieke Doorenbosch and Mike Field (Leiden University). They played an important role in the identification of suitable sections and their sampling. Pollen analyses for sections sampled were performed by Marieke Doorenbosch, while Mike Field studied the plant macro remains. Mike and Erika van Hees aided with the identification and collection of these remains for ^{14}C analysis. Frans Bunnik is acknowledged for placing the Migliaria 44,5 pollen data at our disposal. Wouter van Gorp (RUG) aided with the chemical analysis of the samples, for which we also need to thank Boris Jansen and Sergejus Ustinov from IBED (University of Amsterdam), where most of these analyses were performed. We also thank Wouter van Gorp and Luca Alessandri for the many and fruitful discussions on the dating of the AV layer, which also holds for Johannes van der Plicht and Sanne Palstra from CIO (Groningen University). Mauro di Vito and Ilenia Arienzo from the Osservatorio Vesuviano (INGV) at Napoli are sincerely acknowledged for the fruitful discussions on the potential toxicity of the AV tephra and the dating of this eruption.

Appendix A. Supplementary data

Supplementary data to this article can be found online at https://doi.org/10.1016/j.quageo.2021.101154.

Funding

This work was supported by The Netherlands Organisation for Scientific Research (NWO), Free Competition grant 360-61-060.

References

Van der Plicht, J., Hogg, A., 2006. A note on reporting radiocarbon. Quat. Geochronol. 1 (4), 237–240. https://doi.org/10.1016/j.quageo.2006.07.001.

Albore Livadie, C., 1999. Territorio e insediamenti nell'agro Nolano durante il Bronzo antico (facies di Palma Campania): nota preliminare. In: Albore Livadie, C. (Ed.), L'eruzione vesuviana delle "Pomici di Avellino" e la facies di Palma Campania (Bronzo antico), Atti del Seminario internazionale di Ravello 15-17 luglio 1994. EDIPUGLIA, Bari, pp. 203–245.

Albore Livadie, C., Campajola, L., D'Onofrio, A., Moniot, R., Roca, V., Romano, M., Terrasi, F., 1998. Evidence of the adverse impact of the «Avellino Pumices» eruption of Somma-Vesuvius on old bronze age sites in the Campania region (Southern Italy). Quaternaire 9 (1), 37–43.

Albore Livadie, C., Pearce, M., Delle Donne, M., Pizzano, N., 2019. The effects of the avellino pumice eruption on the population of the early bronze age campanian plain (southern Italy). Quat. Int. 499, 205–220. https://doi.org/10.1016/j.quaint.2018.03.035.

Alessandri, L., 2019. The early and Middle Bronze Age (1/2) in South and central Tyrrhenian Italy and their connections with the Avellino eruption: an overview. Quat. Int. 499, 161–185. https://doi.org/10.1016/j.quaint.2018.08.002.

Arienzo, I., D'Antonio, M., Di Renzo, V., Tonarini, S., Minolfi, G., Orsi, G., Carandente, A., Belviso, P., Civetta, L., 2015. Isotopic microanalysis sheds light on the magmatic endmembers feeding volcanic eruptions: the Astroni 6 case study (Campi Flegrei, Italy). J. Volcanol. Geoth. Res. 304, 24–37. https://doi.org/10.1016/j.jvolgeores.2015.08.003.

Ariztegui, D., Chondrogianni, C., Lami, A., Guilizzoni, P., Lafargue, E., 2001. Lacustrine organic matter and the Holocene paleoenvironmental record of Lake Albano (central Italy). J. Paleolimnol. 26 (3), 283–292. https://doi.org/10.1023/A:1017585808433.

Attema, P., 2017. Sedimentation as geomorphological bias and indicator of agricultural (un)sustainability in the study of the coastal plains of South and Central Italy in antiquity. J. Archaeol. Sci.: For. Rep. 15, 459–469. https://doi.org/10.1016/j.jasrep.2016.07.024.

Ayris, P.M., Delmelle, P., 2012. The immediate environmental effects of tephra emission. Bull. Volcanol. 74, 1905–1936. https://doi.org/10.1007/s00445-012-0654-5.

Bagarinao, T., 1992. Sulfide as an environmental factor and toxicant: tolerance and adaptations in aquatic organisms. Aquat. Toxicol. 24 (1–2), 21–62. https://doi.org/10.1016/0166-445X(92)90015-F.
Bakels, C., Sevink, J., Kuijper, W., Kamermans, H., 2015. The agro Pontino region, refuge after the early bronze age avellino eruption of mount Vesuvius, Italy?. In: Analecta Preahistorica Leidensia, vol. 45 Leiden University, The Netherlands, pp. 55–68.
Balcone-Boissard, H., Boudon, G., Ucciani, G., Villemant, B., Cioni, R., Civetta, L., Orsi, G., 2012. Magma degassing and eruption dynamics of the Avellino pumice Plinian eruption of Somma–Vesuvius (Italy). Comparison with the Pompeii eruption. Earth Planet Sci. Lett. 331, 257–268. https://doi.org/10.1016/j.epsl.2012.03.011.
Banerjee, A., Roychoudhury, A., 2019. Fluorine: a biohazardous agent for plants and phytoremediation strategies for its removal from the environment. Biol. Plant. (Prague) 63 (1), 104–112. https://doi.org/10.32615/bp.2019.013.
Bellotti, P., Calderoni, G., Dall'Aglio, P.L., D'Amico, C., Davoli, L., Di Bella, L., D'Orefice, M., Esu, D., Ferrari, K., Bandini Mazzanti, M., Mercuri, A.M., Tarragoni, C., Torri, P., 2016. Middle-to late-Holocene environmental changes in the Garigliano delta plain (Central Italy): which landscape witnessed the development of the Minturnae Roman colony? Holocene 26 (9), 1457–1471. https://doi.org/10.1177/0959683616640055.
Biserni, G., Van Geel, B., 2005. Reconstruction of Holocene palaeoenvironment and sedimentation history of the Ombrone alluvial plain (South Tuscany, Italy). Rev. Palaeobot. Palynol. 136 (1–2), 16–28. https://doi.org/10.1016/j.revpalbo.2005.04.002.
Boni, C., Bono, P., Calderoni, G., Lombardi, S., Turi, B., 1980. Hydrogeological and geochemical analyses on the relationships between karst circulation and hydrotermal circuit in the Pontina Plain (Southern Latium). Geol. Appl. Idrogeol. 15, 203–245.
Brewer, R., 1964. Fabric and Mineral Analysis of Soils. Wiley, New York, N.Y.
Bronk Ramsey, C., 1995. Radiocarbon calibration and analysis of stratigraphy: the OxCal program. Radiocarbon 37 (2), 425–430. https://doi.org/10.1017/S0033822200033090.
Bronk Ramsey, C., 2009. Bayesian analysis of radiocarbon dates. Radiocarbon 51 (1), 337–360. https://doi.org/10.1017/S0033822200033865.
Bronk Ramsey, C., 2017. OxCal Program, Version 4.3.
Çağatay, M.N., Wulf, S., Sancar, Ü., Özmaral, A., Vidal, L., Henry, P., Appelt, O., Gasperini, L., 2015. The tephra record from the Sea of Marmara for the last ca. 70 ka and its palaeoceanographic implications. Mar. Geol. 361, 96–110. https://doi.org/10.1016/j.margeo.2015.01.005.
Cronin, S.J., Neall, V.E., Lecointre, J.A., Hedley, M.J., Loganathan, P., 2003. Environmental hazards of fluoride in volcanic ash: a case study from Ruapehu volcano, New Zealand. J. Volcanol. Geoth. Res. 121 (3–4), 271–291. https://doi.org/10.1016/S0377-0273(02)00465-1.
Cubellis, E., Marturano, A., Pappalardo, L., 2016. The last Vesuvius eruption in March 1944: reconstruction of the eruptive dynamic and its impact on the environment and people through witness reports and volcanological evidence. Nat. Hazards 82 (1), 95–121. https://doi.org/10.1007/s11069-016-2182-7.
De Haas, T.C., 2011. Fields, Farms and Colonists: Intensive Field Survey and Early Roman Colonization in the Pontine Region, vol. 1. central Italy, Barkhuis.
De Haas, T., 2017. Managing the marshes: an integrated study of the centuriated landscape of the Pontine plain. J, Archaeol. Sci. Rep. 15, 470–481. https://doi.org/10.1016/j.jasrep.2016.07.012.
Dee, M.W., Bronk Ramsey, C., 2014. High-precision Bayesian modeling of samples susceptible to inbuilt age. Radiocarbon 56 (1), 83–94. https://doi.org/10.2458/56.16685.
Dee, M.W., Palstra, S.W.L., Aerts-Bijma, A.T., Bleeker, M.O., De Bruijn, S., Ghebru, F., Jansen, H.G., Kuitems, M., Paul, D., Richie, R.R., Spriensma, J.J., Scifo, A., Van.
Dee, M.W., Wengrow, D., Shortland, A.J., Stevenson, A., Brock, F., Bronk Ramsey, C., 2014. Radiocarbon dating and the Naqada relative chronology. J. Archaeol. Sci. 46, 319–323. https://doi.org/10.1016/j.jas.2014.03.016.
Di Rita, F., Lirer, F., Bonomo, S., Cascella, A., Ferraro, L., Florindo, F., Insigna, D.D., Lurcock, P.C., Margaritelli, G., Petrosino, P., Rettori, R., Vallefuoco, M., Magri, D., 2018. Late Holocene forest dynamics in the Gulf of Gaeta (central Mediterranean) in relation to NAO variability and human impact. Quat. Sci. Rev. 179, 137–152. https://doi.org/10.1016/j.quascirev.2017.11.012.
Di Vito, M.A., Talamo, P., de Vita, S., Rucco, I., Zanchetta, G., Cesarano, M., 2019. Dynamics and effects of the Vesuvius pomici di Avellino plinian eruption and related phenomena on the bronze age landscape of campania region (southern Italy). Quat. Int. 499, 231–244. https://doi.org/10.1016/j.quaint.2018.03.021.
Domene, X., 2016. A critical analysis of meso-and macrofauna effects following biochar supplementation. In: Komang Ralebitso-Senior, T., Orr, C.H. (Eds.), Biochar Application 268-292. Elsevier. https://doi.org/10.1016/B978-0-12-803433-0.00011-4.
Doorenbosch, M., Field, M.H., 2019. A Bronze Age palaeoenvironmental reconstruction from the Fondi basin, southern Lazio, central Italy. Quart. Intern. 499, 221–230. https://doi.org/10.1016/j.quaint.2018.03.022.
Eisenhauer, N., Schuy, M., Butenschoen, O., Scheu, S., 2009. Direct and indirect effects of endogeic earthworms on plant seeds. Pedobiologia 52 (3), 151–162. https://doi.org/10.1016/j.pedobi.2008.07.002.
Feiken, H., 2014. Dealing with Biases: Three Geo-Archaeological Approaches to the Hidden Landscapes of Italy. Barkhuis, Eelde, The Netherlands.
Forey, E., Barot, S., Decaëns, T., Langlois, E., Laossi, K.R., Margerie, P., Scheu, S., Eisenhauer, N., 2011. Importance of earthworm–seed interactions for the composition and structure of plant communities: a review. Acta Oecol. 37 (6), 594–603. https://doi.org/10.1016/j.actao.2011.03.001.
Garand, A., Mucci, A., 2004. The solubility of fluorite as a function of ionic strength and solution composition at 25 C and 1 atm total pressure. Mar. Chem. 91 (1–4), 27–35. https://doi.org/10.1016/j.marchem.2004.04.002.
Grattan, J.P., Pyatt, F.B., 1994. Acid damage to vegetation following the Laki fissure eruption in 1783—an historical review. Sci. Total Environ. 151 (3), 241–247. https://doi.org/10.1016/0048-9697(94)90473-1.
Hansell, A.L., Horwell, C.J., Oppenheimer, C., 2006. The health hazards of volcanoes and geothermal areas. Occup. Environ. Med. 63 (2), 149–156. https://doi.org/10.1136/oem.2005.022459.
Hotes, S., Poschlod, P., Takahashi, H., Grootjans, A.P., Adema, E., 2004. Effects of tephra deposition on mire vegetation: a field experiment in Hokkaido, Japan. J. Ecol. 92, 624–634.
Jouannic, G., Gillot, P.Y., Goiran, J.P., Lefevre, J.C., Siani, G., Salomon, F., Arnoldus-Huyzendveld, A., 2013. Tephrochronological study in the Maccarese lagoon (near Rome, Italy): identification of Holocene tephra layers. Quaternaire. Rev. Assoc. Franç. Ét. Quat. 24 (1), 65–74.
Jung, R., 2017. Chronological problems of the Middle bronze age in southern Italy. In: Lachenal, T., Mordant, J., Nicolas, T., Véber, C. (Eds.), Le Bronze moyen et l'origine du Bronze final en Europe occidentale (XVIIe–XIIIe siècle av. J.-C.). Colloque international de l'APRAB, Strasbourg, 17 au 20 juin 2014, vol. 1. Mém. Archéol. Grand-Est, pp. 623–642.
Koblar, A., Tavčar, G., Ponikvar-Svet, M., 2011. Effects of airborne fluoride on soil and vegetation. J. Fluor. Chem. 132 (10), 755–759. https://doi.org/10.1016/j.jfluchem.2011.05.022.
Kovář, P., Vojtíšek, P., Zentsová, I., 2013. Ants as ecosystem engineers in natural restoration of human made habitats. J. Landsc. Ecol. 6 (1), 18–31. https://doi.org/10.2478/v10285-012-0061-9.
Krauskopf, K.B., 1967. Introduction to Geochemistry. McGraw-Hill, New York.
Kumar, K., Giri, A., Vivek, P., Kalaiyarasan, T., Kumar, B., 2017. Effects of fluoride on respiration and photosynthesis in plants: an overview. J. Environ. Sci. Toxicol. 2 (2) https://doi.org/10.17352/pjest.000011, 043-047.
Lambeck, K., Antonioli, F., Anzidei, M., Ferranti, L., Leoni, G., Scicchitano, G., Silenzi, S., 2011. Sea level change along the Italian coast during the Holocene and projections for the future. Quat. Int. 232 (1), 250–257. https://doi.org/10.1016/j.quaint.2010.04.026.
Magny, M., De Beaulieu, J.L., Drescher-Schneider, R., Vannière, B., Walter-Simonnet, A. V., Miras, Y., Millet, L., Bossuet, G., Peyron, O., Brugiapaglia, E., Leroux, A., 2007. Holocene climate changes in the central Mediterranean as recorded by lake-level fluctuations at Lake Accesa (Tuscany, Italy). Quat. Sci. Rev. 26 (13–14), 1736–1758. https://doi.org/10.1016/j.quascirev.2007.04.014.
Maher Jr., L.J., 1972. Absolute pollen diagram of redrock lake, boulder county, Colorado. Quat. Res. (Orlando) 2 (4), 531–553. https://doi.org/10.1016/0033-5894(72)90090-7.
Majer, J.D., Brennan, K.E., Bisevac, L., 2008. Terrestrial invertebrates. In: Perrow, M.R., Davy, A.J. (Eds.), Handbook of Ecological Restoration: Volume 1, Principles of Restoration. Cambridge University Press, Cambridge, UK, pp. 279–299. https://doi.org/10.1017/CBO9780511549984.017.
Margaritelli, G., Vallefuoco, M., Di Rita, F., Capotondi, L., Bellucci, L.G., Insinga, D.D., Petrosino, P., Bonomo, S., Cacho, I., Cascella, A., Ferraro, L., Florindo, F., Lubritto, C., Lurcock, P.C., Magri, D., Pelosi, N., Rettori, R., Lirer, F., 2016. Marine response to climate changes during the last five millennia in the central Mediterranean Sea. Global Planet. Change 142, 53–72. https://doi.org/10.1016/j.gloplacha.2016.04.007.
McBride, M.B., 1994. Environmental Chemistry of Soils. Oxford University Press, Oxford, UK.
Mook, W.G., Van Der Plicht, J., 1999. Reporting ^{14}C activities and concentrations. Radiocarbon 41 (3), 227–239. https://doi.org/10.1017/S0033822200057106.
Passariello, I., Livadie, C.A., Talamo, P., Lubritto, C., D'Onofrio, A., Terrasi, F., 2009. 14 C chronology of Avellino Pumices eruption and timing of human reoccupation of the devastated region. Radiocarbon 51 (2), 803–816. https://doi.org/10.1017/S0033822200056113.
Passariello, I., Lubritto, C., D'Onofrio, A., Guan, Y., Terrasi, F., 2010. The somma–vesuvius complex and the phlaegrean fields caldera: new chronological data of several eruptions of the copper–middle bronze age period. Nucl. Instrum. Methods Phys. Res. Sect. B Beam Interact. Mater. Atoms 268 (7–8), 1008–1012.
Petrone, P., Giordano, M., Giustino, S., Guarino, F.M., 2011. Enduring fluoride health hazard for the Vesuvius area population: the case of AD 79 Herculaneum. PloS One 6 (6), e21085. https://doi.org/10.1371/journal.pone.0021085.
Ramrath, A., Zolitschka, B., Wulf, S., Negendank, J.F., 1999. Late Pleistocene climatic variations as recorded in two Italian maar lakes (Lago di Mezzano, Lago Grande di Monticchio). Quat. Sci. Rev. 18 (7), 977–992. https://doi.org/10.1016/S0277-3791(99)00009-8.
Razum, I., Miko, S., Ilijanić, N., Petrelli, M., Röhl, U., Hasan, O., Giaccio, B., 2020. Holocene tephra record of Lake Veliko jezero, Croatia: implications for the central Mediterranean tephrostratigraphy and sea level rise. Boreas. https://doi.org/10.1111/bor.12446.
Robins, R., Robins, A., 2011. The antics of ants: ants as agents of bioturbation in a midden deposit in south-east Queensland. Environ. Archaeol. 16 (2), 151–161. https://doi.org/10.1179/174963111X13110803261010.
Sappa, G., Ergul, S., Ferranti, F., 2014. Water quality assessment of carbonate aquifers in southern Latium region, Central Italy: a case study for irrigation and drinking purposes. Appl. Water Sci. 4 (2), 115–128. https://doi.org/10.1007/s13201-013-0135-9.
Sevink, J., 2020. Burnt clay or *terra bruciata* in coastal basins of Southern Lazio: evidence for prehistoric *ignicoltura* or resulting from drainage of Holocene pyritic sediments? J. Archaeol. Sci., Rep. https://doi.org/10.1016/j.jasrep.2020.102432.

Sevink, J., Remmelzwaal, A., Spaargaren, O.C., 1984. The soils of southern Lazio and adjacent campania. Publ. Fys. Geogr. Lab. UvA Nr. 38. University of Amsterdam, The Netherlands.

Sevink, J., Vos, P., Westerhoff, W.E., Stierman, A., Kamermans, H., 1982. A sequence of marine terraces near Latina (Agro Pontino, Central Italy). Catena 9 (3–4), 361–378. https://doi.org/10.1016/0341-8162(82)90010-8.

Sevink, J., Van Bergen, M.J., Van der Plicht, J., Feiken, H., Anastasia, C., Huizinga, A., 2011. Robust date for the Bronze age avellino eruption (Somma-Vesuvius): 3945 ± 10 calBP (1995 ± 10 calBC). Quat. Sci. Rev. 30, 1035–1046. https://doi.org/10.1016/j.quascirev.2011.02.001.

Sevink, J., Van der Plicht, J., Feiken, H., Van Leusen, P.M., Bakels, C.C., 2013. The Holocene of the Agro Pontino graben: recent advances in its palaeogeography, palaeoecology, and tephrostratigraphy. Quat. Int. 303, 153–162. https://doi.org/10.1016/j.quaint.2013.01.006.

Sevink, J., De Neef, W., Vito, M.A.D., Arienzo, I., Attema, P.A.J., van Loon, E.E., Burkhart, U., Den Haan, M., Ippolito, F., Noorda, N., 2020a. A multidisciplinary study of an exceptional prehistoric waste dump in the mountainous inland of Calabria (Italy): implications for reconstructions of prehistoric land use and vegetation in Southern Italy. Holocene 1310–1331. https://doi.org/10.1177/0959683620919974.

Sevink, J., Van Gorp, W., Di Vito, M.A., Arienzo, I., 2020b. Distal tephra from campanian eruptions in early late Holocene fills of the agro Pontino graben and Fondi basin (southern Lazio, Italy). J. Volcanol. Geoth. Res. https://doi.org/10.1016/j.jvolgeores.2020.107041.

Signorelli, S., Vaggelli, G., Romano, C., 1999. Pre-eruptive volatile (H_2O, F, Cl and S) contents of phonolitic magmas feeding the 3550-year old Avellino eruption from Vesuvius, southern Italy. J. Volcanol. Geoth. Res. 93 (3), 237–256. https://doi.org/10.1016/S0377-0273(99)00117-1.

Smith, V.C., Isaia, R., Pearce, N.J.G., 2011. Tephrostratigraphy and glass compositions of post-15 kyr Campi Flegrei eruptions: implications for eruption history and chronostratigraphic markers. Quat. Sci. Rev. 30 (25–26), 3638–3660. https://doi.org/10.1016/j.quascirev.2011.07.012.

Sulpizio, R., Bonasia, R., Dellino, P., Di Vito, M.A., La Volpe, L., Mele, D., Zanchetta, G., Sadori, L., 2008. Discriminating the long distance dispersal of fine ash from sustained columns or near ground ash clouds: the example of the Pomici di Avellino eruption (Somma-Vesuvius, Italy). J. Volcanol. Geoth. Res. 177 (1), 263–276.

Sulpizio, R., Welden, A.V., Caron, B., Zanchetta, G., 2010. The Holocene tephrostratigraphic record of Lake Shkodra (Albania and Montenegro). J. Quat. Sci. 25 (5), 633–650. https://doi.org/10.1002/jqs.1334.

Sundelin, B., Eriksson, A.K., 2001. Mobility and bioavailability of trace metals in sulfidic coastal sediments. Environ. Toxicol. Chem. 20 (4), 748–756. https://doi.org/10.1002/etc.5620200408.

Tuccimei, P., Salvati, R., Capelli, G., Delitala, M.C., Primavera, P., 2005. Groundwater fluxes into a submerged sinkhole area, Central Italy, using radon and water chemistry. Appl. Geochem. 20 (10), 1831–1847. https://doi.org/10.1016/j.apgeochem.2005.04.006.

Vacchi, M., Marriner, N., Morhange, C., Spada, G., Fontana, A., Rovere, A., 2016. Multiproxy assessment of Holocene relative sea-level changes in the western Mediterranean: sea-level variability and improvements in the definition of the isostatic signal. Earth Sci. Rev. 155, 172–197. https://doi.org/10.1016/j.earscirev.2016.02.002.

Van Gorp, W., Sevink, J., 2019. Distal deposits of the avellino eruption as a marker for the detailed reconstruction of the early bronze age depositional environment in the agro Pontino and Fondi basin (Lazio, Italy). Quat. Int. 499, 245–257. https://doi.org/10.1016/j.quaint.2018.03.017.

Van Gorp, W., Sevink, J., Van Leusen, M., 2020. The role of subsidence in Early Bronze Age lake and sea level reconstruction in the Agro Pontino (Lazio, Italy) over the last 4ka using the Avellino tephra marker bed. Catena 194. https://doi.org/10.1016/j.catena.2020.104770.

Van Joolen, E., 2003. Archaeological Land Evaluation. A Reconstruction of the Suitability of Ancient Landscapes for Various Land Uses in Italy Focused on the First Millennium BC. PhD thesis. University of Groningen, The Netherlands.

Van Mourik, J.M., 1999. The use of micromorphology in soil pollen analysis; the interpretation of the pollen content of slope deposits in Galicia, Spain. Catena 35, 239–257. https://doi.org/10.1016/S0341-8162(98)00103-9.

Vanzetti, A., Marzocchella, A., Saccoccio, F., 2019. The Campanian agrarian systems of the late Copper-Early Bronze Age (ca. 4550-3850 cal BP): a long-lasting agrarian management tradition before the Pomici di Avellino eruption. Quat. Int. 499, 148–160. https://doi.org/10.1016/j.quaint.2018.09.034.

Wagner, B., Sulpizio, R., Zanchetta, G., Wulf, S., Wessels, M., Daut, G., Nowaczyk, N., 2008. The last 40 ka tephrostratigraphic record of Lake Ohrid, Albania and Macedonia: a very distal archive for ash dispersal from Italian volcanoes. J. Volcanol. Geoth. Res. 177 (1), 71–80. https://doi.org/10.1016/j.jvolgeores.2007.08.018.

Weinstein, L.H., Davison, A., 2004. Fluorides in the Environment: Effects on Plants and Animals. Cabi, Wallingford, UK.

Wulf, S., Kraml, M., Brauer, A., Keller, J., Negendank, J.F., 2004. Tephrochronology of the 100 ka lacustrine sediment record of Lago Grande di Monticchio (southern Italy). Quat. Int. 122 (1), 7–30. https://doi.org/10.1016/j.quaint.2004.01.028.

Zanchetta, G., Sulpizio, R., Roberts, N., Cioni, R., Eastwood, W.J., Siani, G., Caron, B., Paterne, M., Santacroce, R., 2011. Tephrostratigraphy, chronology and climatic events of the Mediterranean basin during the Holocene: an overview. Holocene 21 (1), 33–52. https://doi.org/10.1177/0959683610377531.

Zanchetta, G., Bini, M., Di Vito, M.A., Sulpizio, R., Sadori, L., 2019. Tephrostratigraphy of paleoclimatic archives in central mediterranean during the bronze age. Quat. Int. 499, 186–194. https://doi.org/10.1016/j.quaint.2018.06.012.